

History 1/4

Volume 4, number 3

PHYSICS LETTERS

1 April 1963

- 1) R. Rabinowitz et al., Proc. Inst. Radio Engrs. (correspondence) 50 (1962) 2365.
- 2) A. Javan, E. A. Ballik and W. L. Bond, J. Opt. Soc. Am. 52 (1962) 96.
- 3) S. Jacobs and P. Rabinowitz, Proc. of the 3rd Quantum Electronics Conf., Paris, 1963 (to be published).

- 4) K. D. Froome and R. H. Bradwell, J. Sci. Instr. 38 (1961) 458.
- 5) J. Terrien, J. phys. radium 19 (1958) 390.
- 6) G. R. Hanes, Can. J. Phys. 37 (1959) 1283.
- 7) C. F. Bruce and R. M. Hill, Australian J. Phys. 14 (1961) 64; 15 (1962) 152.
- 8) R. M. Hill and C. F. Bruce, Australian J. Phys. 15 (1962) 194.

THE COMPTON EFFECT ON RELATIVISTIC ELECTRONS AND THE POSSIBILITY OF OBTAINING HIGH ENERGY BEAMS

F. R. ARUTYUNIAN and V. A. TUMANIAN
Physical Institute of the State Committee of the Council of Ministers of the USSR for the Use of Atomic Energy

Received 20 February 1963

A characteristic feature of the Compton effect on relativistic electrons is the appearance of photons with energies exceeding those of the primary photons. As a result, even when light photons are scattered on extremely relativistic electrons, the energies of the scattered photons will be of the same order of magnitude as those of the electrons. This feature may possibly be exploited for obtaining high energy γ -ray beams in electron accelerators. An important point to be mentioned is that the characteristics of such γ -beams will significantly differ from those obtained by bremsstrahlung.

In the Compton effect involving moving electrons the energy of the scattered quantum ω_2 is related to the energy of the primary photon ω_1 by the well known equation ($\hbar = c = 1$)

$$\omega_2 = \omega_1 \frac{1 - v_1 \cos \theta_1}{1 - v_1 \cos \theta_2 + (\omega_1/\epsilon_1)(1 - \cos \theta)}, \quad (1)$$

where v_1 and ϵ_1 are respectively the electron velocity and energy, θ_1 and θ_2 are the angles between the direction of motion of the electrons and incident and scattered quanta and θ is the angle between the incident and scattered quanta. The energy of the scattered γ -quanta is maximal ($\omega_2 \text{ max}$) when the primary electron and photon move in opposite directions ($\theta_1 = \pi$) and the scattered photon moves in the direction of the electron. Then ($v_1 = 1$)

$$\omega_2 \text{ max} = \frac{2\omega_1}{1 + (m/\epsilon_1)^2 + 2\omega_1/\epsilon_1}, \quad (2)$$

where m is the electron rest energy.

The highest energy to attain possibly in electron accelerators in the near future should be ~ 6 GeV.

Of course in order to obtain γ -beams by the method considered here high photon fluxes will be required. A high intensity photon source that should be feasible is the laser. At present ruby lasers seem to be the most reliable.

For ruby laser photons ($\lambda = 6943 \text{ \AA}$) scattered on 6 GeV electrons one gets $\omega_2 \text{ max} = 848 \text{ MeV}$. This effect rapidly grows with increase of the electron energy. Thus for the same ruby lasers and $\epsilon_1 = 40$ and 500 GeV the maximal energy is corresponding $\omega_2 \text{ max} \sim 21$ and 497 GeV.

Of course if lasers emitting shorter wavelengths or other sources of high energy photons be employed, the energies of the scattered photons may closely approach those of the electrons.

The differential cross section for Compton scattering on moving electrons is (1)

$$d\sigma = r_0^2 \frac{2}{m^2} \frac{1}{x_1^2} \left\{ \frac{1}{x_1} + \frac{1}{x_2} \right\}^2 - 4 \left(\frac{1}{x_1} + \frac{1}{x_2} \right) - \left(\frac{x_1}{x_2} + \frac{x_2}{x_1} \right) \left\{ \omega_2^2 \frac{d\Omega_2}{2} \right\}, \quad (3)$$

where r_0 is the classical electron radius and

$$x_1 = -\frac{2\omega_1}{m^2} (\epsilon_1 + P_1),$$

$$x_2 = \frac{2\omega_2}{m^2} (\epsilon_1 - P_1 \cos \theta_2),$$

where P_1 is the electron momentum.

The energy spectrum of the scattered photons can be derived from expressions (3) and (1). Neglecting small terms in (3) we obtain

PHYSICAL REVIEW LETTERS

VOLUME 10

1 FEBRUARY 1963

NUMBER 3

ELECTRON SCATTERING BY AN INTENSE POLARIZED PHOTON FIELD*

Richard H. Milburn
Department of Physics, Tufts University, Medford, Massachusetts
(Received 26 December 1962)

Compton scattering by starlight quanta has been postulated by Feenberg and Primakoff to be a mechanism for the energy degradation of high-energy electrons in interstellar space.¹ We shall discuss here the possibility of observing this phenomenon directly in the laboratory by scattering a multi-GeV electron beam against the intense flux of visible photons produced by a typical laser. It will be shown that using existing laser systems and electron accelerators, one may expect to obtain the order of several thousand collimated high-energy scattered photons during each accelerator pulse, and that these quanta retain to a high degree the polarization of the original beam of optical photons.

The kinematic formulas for Compton scattering on moving electrons are given by Feenberg and Primakoff.² We shall consider the special case of an extreme-relativistic electron of energy $E = \gamma mc^2$, $\gamma = 1/(1 - \beta^2)^{1/2} \gg 1$, incident head-on upon a beam of photons of energy $k_i = (1-3) \text{ eV}$ propagating in the opposite direction. An observer moving with the incident electron will see a photon of energy $k_o = 2\gamma k_i$. In Table I are listed for various laboratory electron energies, E , the corresponding values of k_o , tabulated in terms of $\lambda = k_o/mc^2$, for incident 6943 \AA ruby-laser photons ($k_i = 1.79 \text{ eV}$). If we let θ_o equal the photon scattering angle in the electron rest frame, and $x = \cos \theta_o$, then the laboratory energy of the scattered photon will be given approximately by

$$k_f = E[\lambda(1-x)/[1 + \lambda(1-x)]]. \quad (1)$$

The approximation falls only near $x = 1$, for which $k_f = k_i$ is required. However, for large $\gamma = E/mc^2$ the bulk of the scattered photons is folded back and emerges in the laboratory in the direction of motion of the incident electron, making angles with that direction given by $\theta = 2 \tan^{-1}(\beta) = (1/\gamma) \times \cot^{-1}(\beta)$. Thus for 1-GeV electrons, all photons having $23^\circ < \theta_o < 180^\circ$ will end up within 0.0025 radian of the electron direction. We shall confine our discussion to these high-energy quanta. The

Table I. Energy, λ , polarization, and cross section for highest energy photons produced by ruby-laser photons scattered on electrons of energy E . The quantity $\sigma_{1/2}$ is the cross section for higher half of k_f spectrum.

E (GeV)	λ	$(k_f)_{\text{max}}$ (MeV)	P_{max}	$\sigma_{1/2}$ (mb)
1.02	0.014	28	1.00	320
2.92	0.040	216	1.00	310
4.16	0.057	426	0.99	300
4.60	0.063	515	0.99	290
5.11	0.070	628	0.99	290
5.48	0.075	715	0.99	290
5.84	0.080	806	0.99	280
6.21	0.085	903	0.99	280
6.57	0.090	1.00 $\times 10^3$	0.99	280
8.76	0.120	1.69 $\times 10^3$	0.98	260
11.69	0.160	2.63 $\times 10^3$	0.96	250
20.8	0.295	7.55 $\times 10^3$	0.91	220
41.6	0.570	22.1 $\times 10^3$	0.77	180
58.4	0.800	35.9 $\times 10^3$	0.67	160

75

176

6/26/09

Carlo Schaerf Yerevan 1/06/09

1

History 2/4

1963 F.R. Arutyunyan and V.A. Tumanian, Phys. Lett. 4 (1963), 176; Sov. Phys. Usp. 83 (1964), 339;

R. H. Milburn, Phys. Rev. Lett. 10 (1963) 75.

Have shown that backward scattering of Laser light against high energy electrons can produce high-energy γ -rays.

1964-1969 O.F. Kulikov et al., Phys. Lett. 13 (1964), 344;

C. Bemporad et al., Phys. Rev. 138B (1965), 1546;

J. Ballam et al., Phys. Rev. Lett. 23 (1969), 498.

Have employed this technique in several laboratories (Lebedev Institute, CEA, SLAC) obtaining low flux of γ -rays (10-100 γ /s).

1967 R. Malvano, C. Mancini and C. Schaerf, LNF - 67/48 (1967)

Pointed out that, by exploiting the power inside laser cavities and the intense electron beams that circulate in storage rings, one could produce intense polarized gamma-ray beams for photonuclear-reaction experiments.

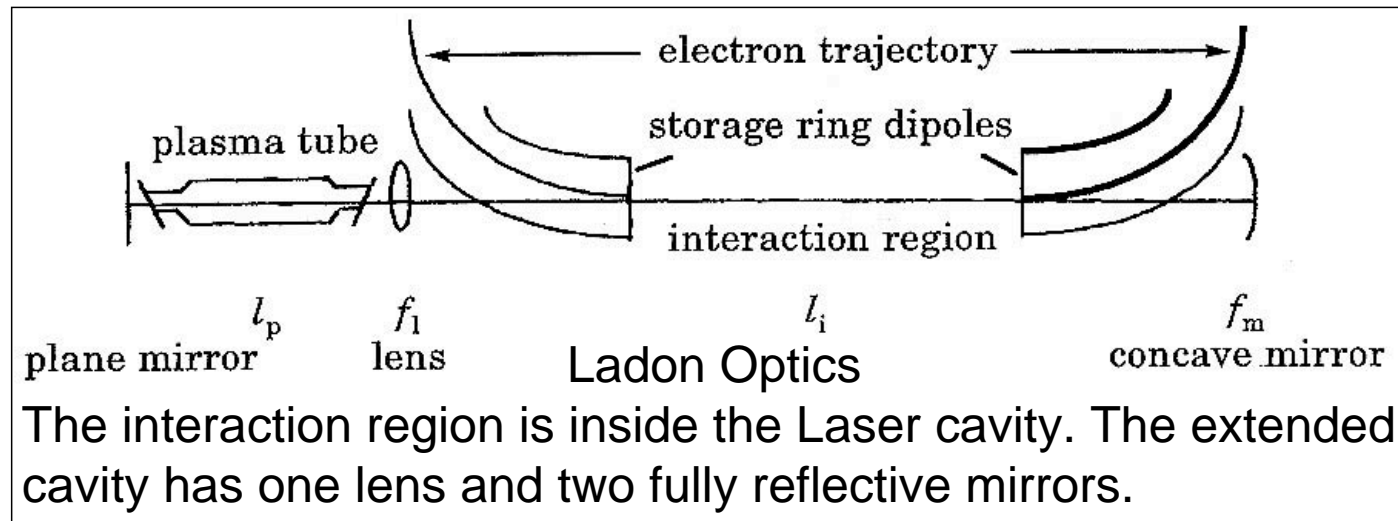
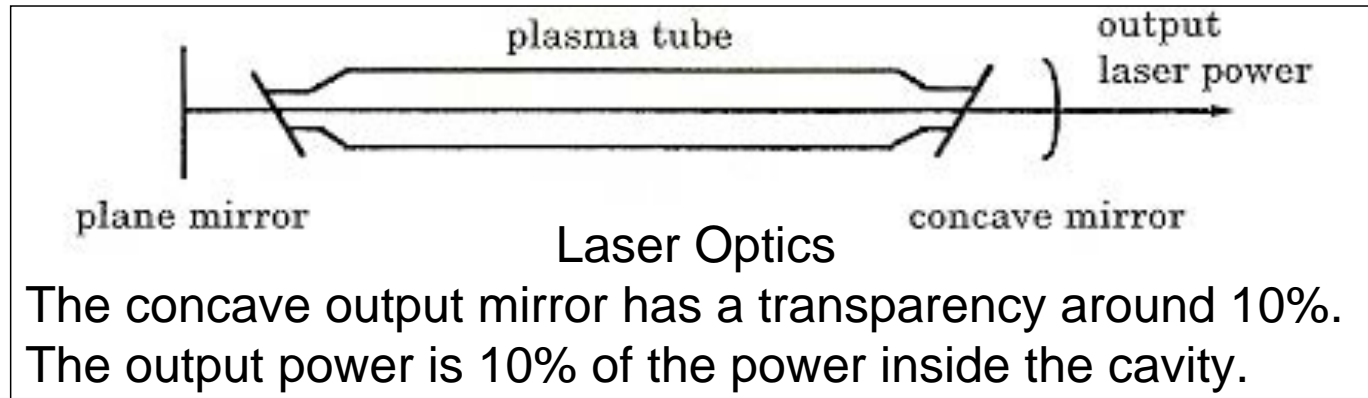
1978 L. Casano et al., Laser and Unconventional Optics Journal 55, 3 (1975);

G. Matone et al., Lecture Notes in Physics 62 (1977), 149;

L. Federici et al., Nuovo Cimento 59B (1980), 247.

Have produced the first Compton Backscattering γ -ray beam by the interaction of the electrons **circulating in a storage ring** with the high intensity photons **available inside a Laser cavity**.

History 3/4



History 4/4

The first backscattered beam was built on **Adone**, Frascati's successor to the original ADA, the first e^+e^- storage ring. The generic name "Ladon beams" now used for such gamma sources not only honours the Adone ring; it also recalls the River Ladon of Greek mythology ^[1].

Following the early successes at Adone, Ladon beams were built at several other storage rings. Three Ladon beams were built in the Novosibirsk laboratory in Russia. They were good beams but their use was spoiled, first by an accidental fire that destroyed much of the laboratory and then by the demise of the Soviet Union. Table I lists ROKK-1M, the third of the Novosibirsk Ladon beams, and others around the world.

Four of them — **LEGS** ^[2] in the USA, **Graal** ^[3] in France, **LEPS** in Japan, and **HIGS** in the USA — have been in operation for many years. Collectively, they have covered the gamma-ray spectrum from a few MeV all the way up to 2.4 GeV.

LEGS and **Graal** have been decommissioned in 2007 and 2008 respectively and now the only remaining in operation are **LEPS** and **HIGS**.

1. Λαδων "riviere de Grece, au Péloponnèse dans l'Arcadie. ... les Mythologistes firent le Ladon pere de la nymphe Daphné & de la nymphe Syrinx. Il étoit couvert de magnifiques roseaux, dont Pan se servit pour sa flûte á sept tuyaux." (M. Diderot and M. D'Alembert, Encyclopédie, a Paris MDCCLVII).
2. A.M. Sandorfi, M.J. Le Vine, C.E. Thorn, G. Giordano, G. Matone and C. Schaerf: HIGH ENERGY GAMMA RAY BEAMS FROM COMPTON BACKSCATTERED LASER LIGHT -IEEE Trans. on Nucl. Science, NS-30/4, 3083 (1983).
3. R. Caloi, L. Casano, M.P. DePascale, L. Federici, S. Frullani, B. Girolami, G. Giordano, G. Matone, M. Mattioli, G. Pasquariello, P. Pelfer, P. Picozza, E. Poldi, D. Prospero and C. Schaerf: THE LADON PHOTON BEAM WITH THE ESRF-5 GEV MACHINE. Lettere al Nuovo Cimento, 27, 339 (1980).

Ladon Beams Table

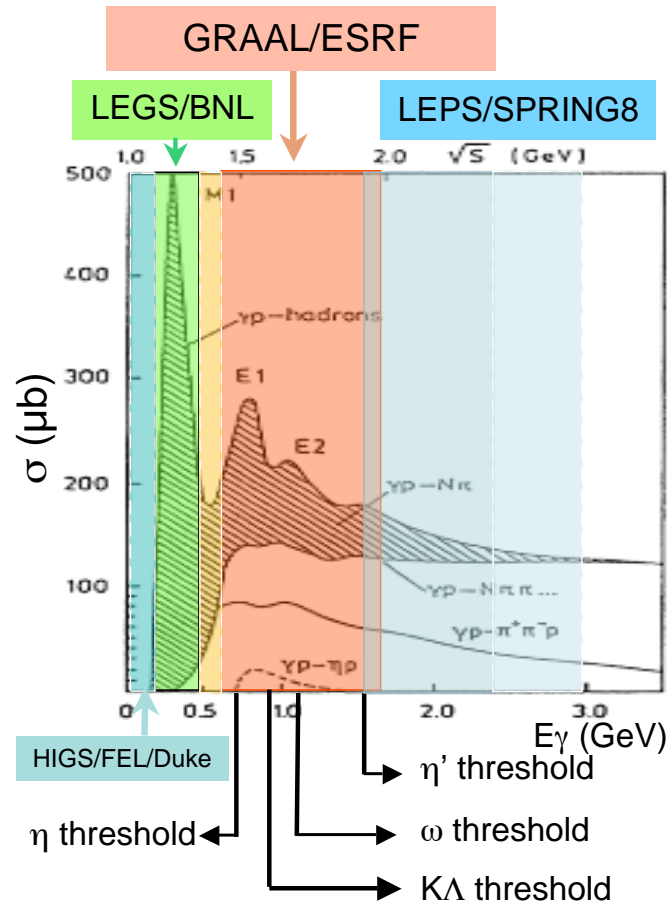
TABLE I

Project name	Ladon ^o	Taladon ⁺	ROKK ^Δ -1M	LEGS [*]	LEGS-2	Graal ^{**}	LEPS [†]	HIGS [⊙]	
Location	Frascati (LNF-INFN)		Novosibirsk	Brookhaven (BNL)		Grenoble	Harima	Durham	
Storage ring	Adone	Adone	VEPP-4M	NSLS	NSLS	ESRF	SPring-8	TUNL-FELL	
Energy defining method	collimation	internal tagging	tagging	external tagging	external tagging	internal tagging	internal tagging	collimation	
Electron energy	GeV	1.5	1.5	1.4 - 5.3	2.5	2.8	6.04	8	1.0
Photon energy	eV	2.45	2.45	1.17-3.51	3.53	4.71	3.53	3.53	8.2
Gamma-ray energy	MeV	5-80	35-80	100-1200	180-320	285-470	550-1470	1500-2400	5-95
		variable	simultaneous						variable
Energy resolution	%	1.4-10	5	--	1.6	1.1	1.1	1.25	1
(FWHM)	MeV	0.07-8	4-2	--	5	5	16	30	
Electron current	A	0.1	0.1	0.1	0.2	0.2	0.2	0.1	100
Gamma intensity	s ⁻¹	10 ⁵	5 10 ⁵	2 10 ⁶	4 10 ⁶	2 10 ⁶	2 10 ⁶	2 10 ⁶	10 ⁶ -10 ⁸
Years of operation		1978-1989	1989-1993	1993	1987-1999	1999-2007	1996-2008	1999	1999

^o Laser ADONe, ⁺Tagged LADON, ^ΔROKK is a russian abbreviation for Backscattered Compton Gamma, ^{*} Laser Electron Gamma Source, ^{**} GRenoble Anneau Accelérateur Laser, [⊙] High Intensity Gamma-ray Source, [†] Laser-Electron Photons at SPring-8

Λαδων "riviere de Grece, au Péloponnèse dans l'Arcadie. ... les Mythologistes firent le Ladon pere de la nymphe Daphné & de la nymphe Syrinx. Il étoit couvert de magnifiques roseaux, dont Pan se servit pour sa flûte à sept tuyaux." (M. Diderot and M. D'Alembert, Encyclopédie, a Paris MDCCLVII).

Ladon Beams in the World

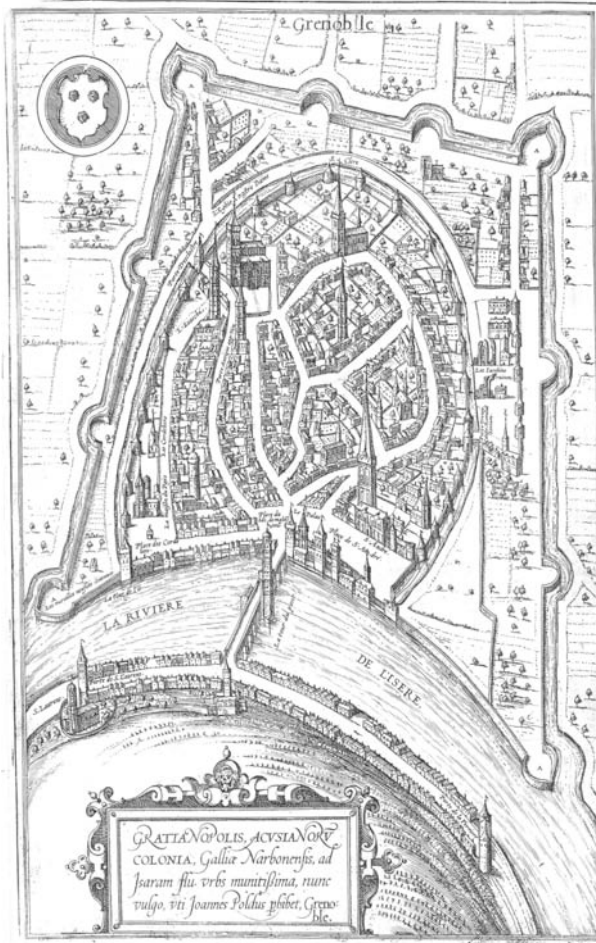


- Graal:
- $E_\gamma = .6-1.5 \text{ GeV} / W=1.4-1.9 \text{ GeV}$
- Region of the second and third baryon resonances
- η, K, ω, η' thresholds
- Complementary of HIGS, LEGS, Graal and LEPS

The ESRF at Grenoble from Satelite



Gratianopolis 1572



6/26/09

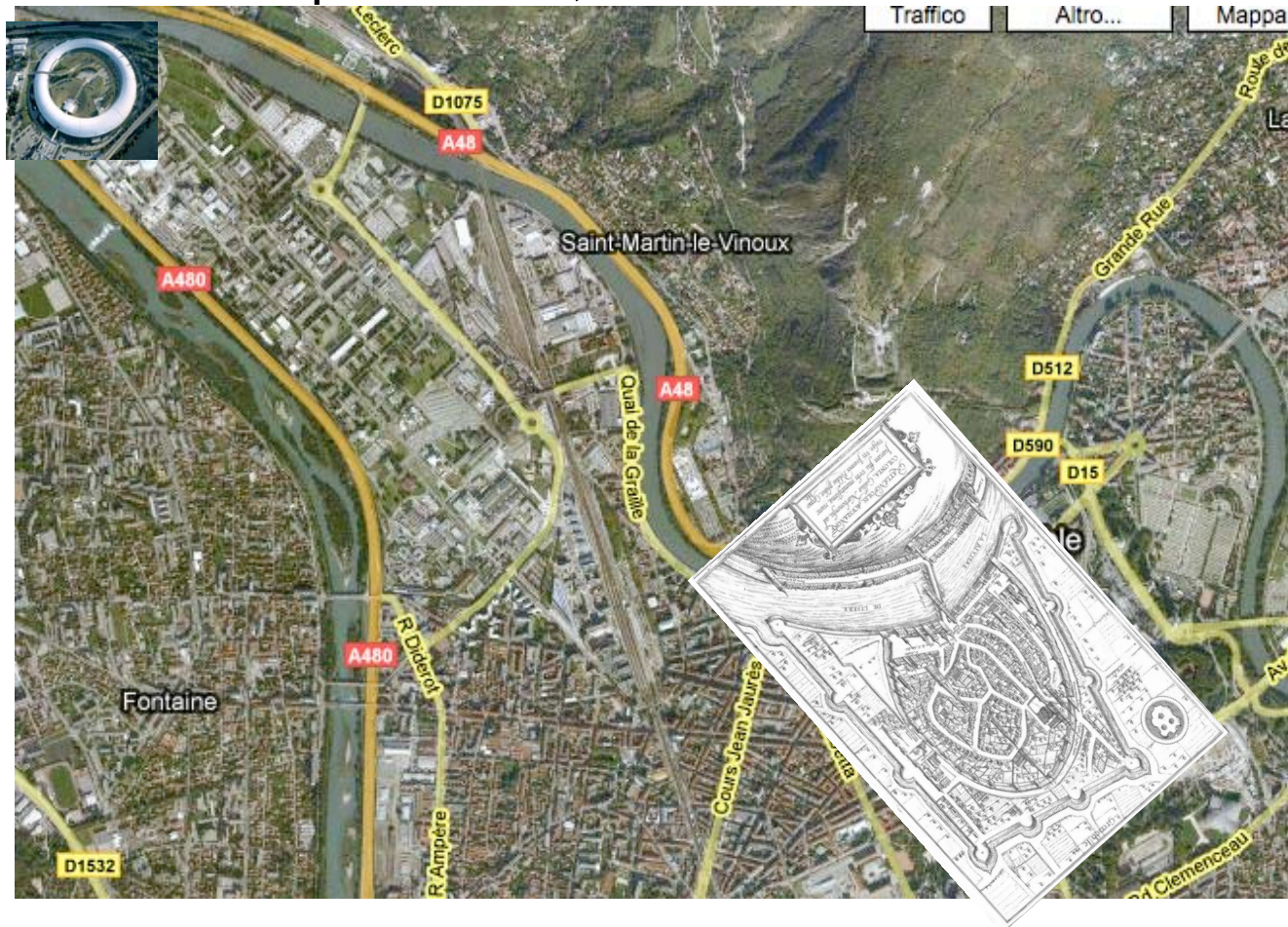
ESRF 2004



Carlo Schaerf Yerevan 1/06/09

8

Gratianopolis 1572, Grenoble and the ESRF

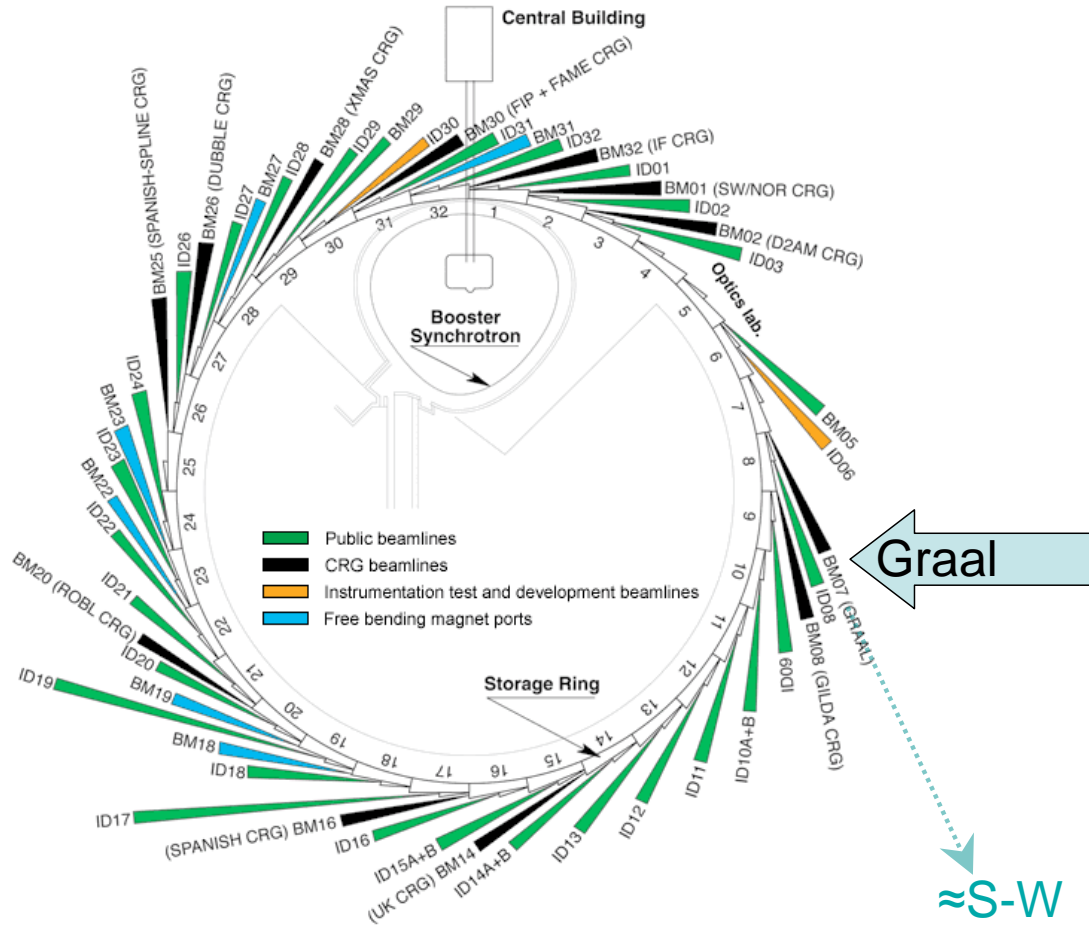


6/26/09


Carlo Schaerf Yerevan 1/06/09


9

The ESRF Beamlines



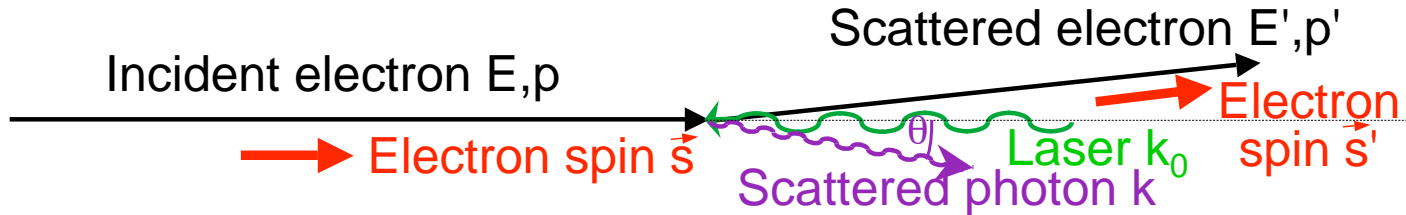
The ESRF Electron Beam

Energy	GeV	6.03
Maximum Current	mA	200
Horizontal Emittance	nm	 $\epsilon_x = 4$
Vertical Emittance (*minimum achieved)	nm	0.025 (0.010*)
Coupling (*minimum achieved)	%	0.6 (0.25*)
Revolution frequency	kHz	355
Number of bunches		1 to 992
Time between bunches	ns	2816 to 2.82

Filling pattern bunch	Uniform	16-bunch	Single
Maximum current (mA)	200	90	20
Lifetime (hours)	75	9	6
Rms energy spread (%)	 $\sigma_p = 0.11$	0.12	0.22
Rms bunch length (ps)	20	48	73

64 bending magnets, 320 quadrupoles, 224 sextupoles.
 RF 352.2 MHz, T=2.839 ns.

Kinematics of Electron-photon In-flight Scattering

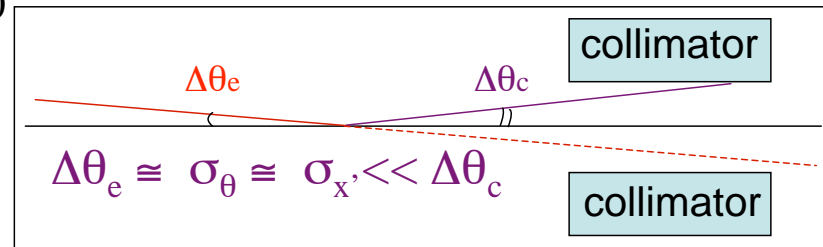


$$k_{\max} = \frac{4\gamma^2 k_0}{1 + \frac{4\gamma k_0}{m_e}}; \quad \gamma = \frac{E}{m_e} \approx 11800; \quad k = \frac{4\gamma^2 k_0}{1 + \frac{4\gamma k_0}{m_e} + (\gamma\theta)^2}; \quad \gamma\theta \ll 1;$$

$$\Delta\theta \geq \Delta\theta_e \equiv \sigma_{\theta_e} \equiv \sigma_{x'} \equiv \sqrt{\frac{\varepsilon_x}{\beta_x}} \equiv \sqrt{\frac{4 \cdot 10^{-9}}{30}} = 1.15 \cdot 10^{-5}$$

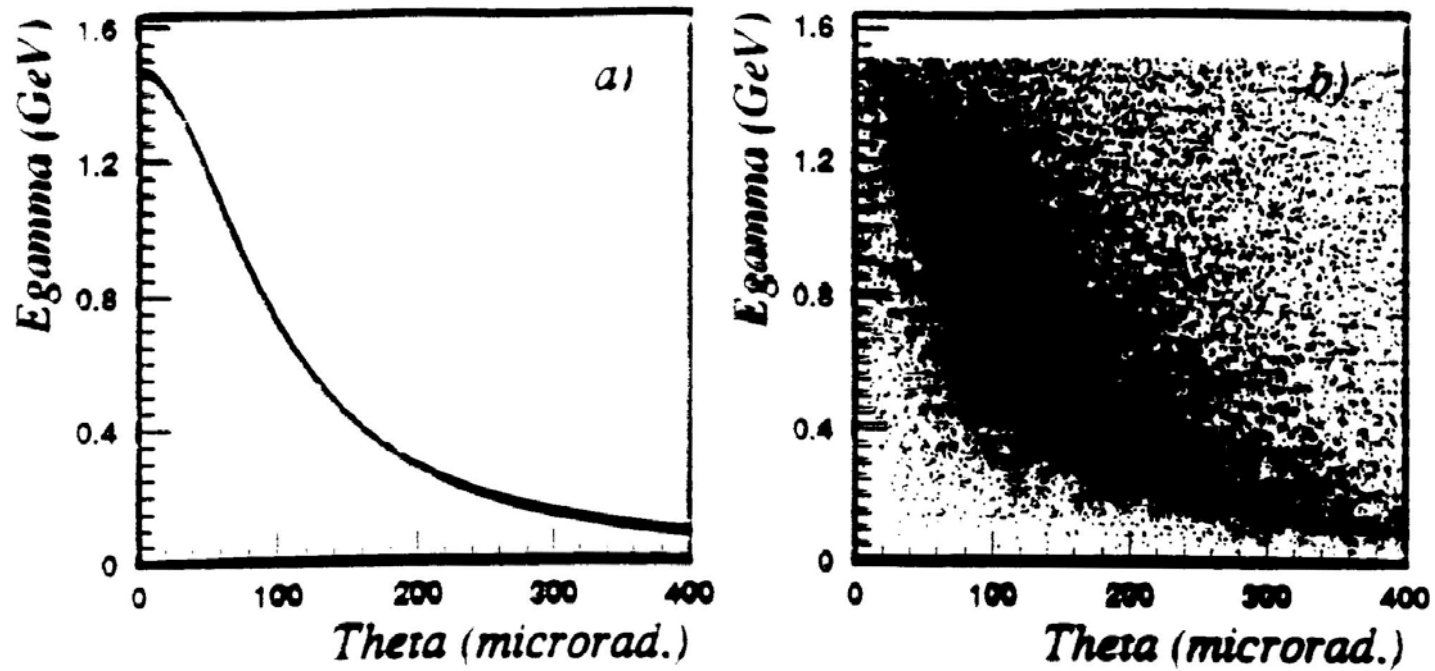
$$\gamma \Delta\theta_e \approx 11800 \cdot 1.15 \cdot 10^{-5} = 0.14$$

$$\frac{\vec{s} \cdot \vec{p}}{p} = \frac{\vec{s}' \cdot \vec{p}'}{p'}$$



At these very high energies the electron helicity is conserved and there is no transfer of spin angular momentum from the electron to the photon, therefore the polarization of the highest energy gamma-rays (scattered at 180°) is the same as that of the laser photons.

Kinematics of Electron-photon In-flight Scattering



Kinematics of Electron-photon In-flight Scattering

Tagging: $k = E + k_0 - E' \approx E - E'$; $\sigma_k^2 = \sigma_E^2 + \sigma_{E'}^2$ ($\bar{\tau}$ correlations)

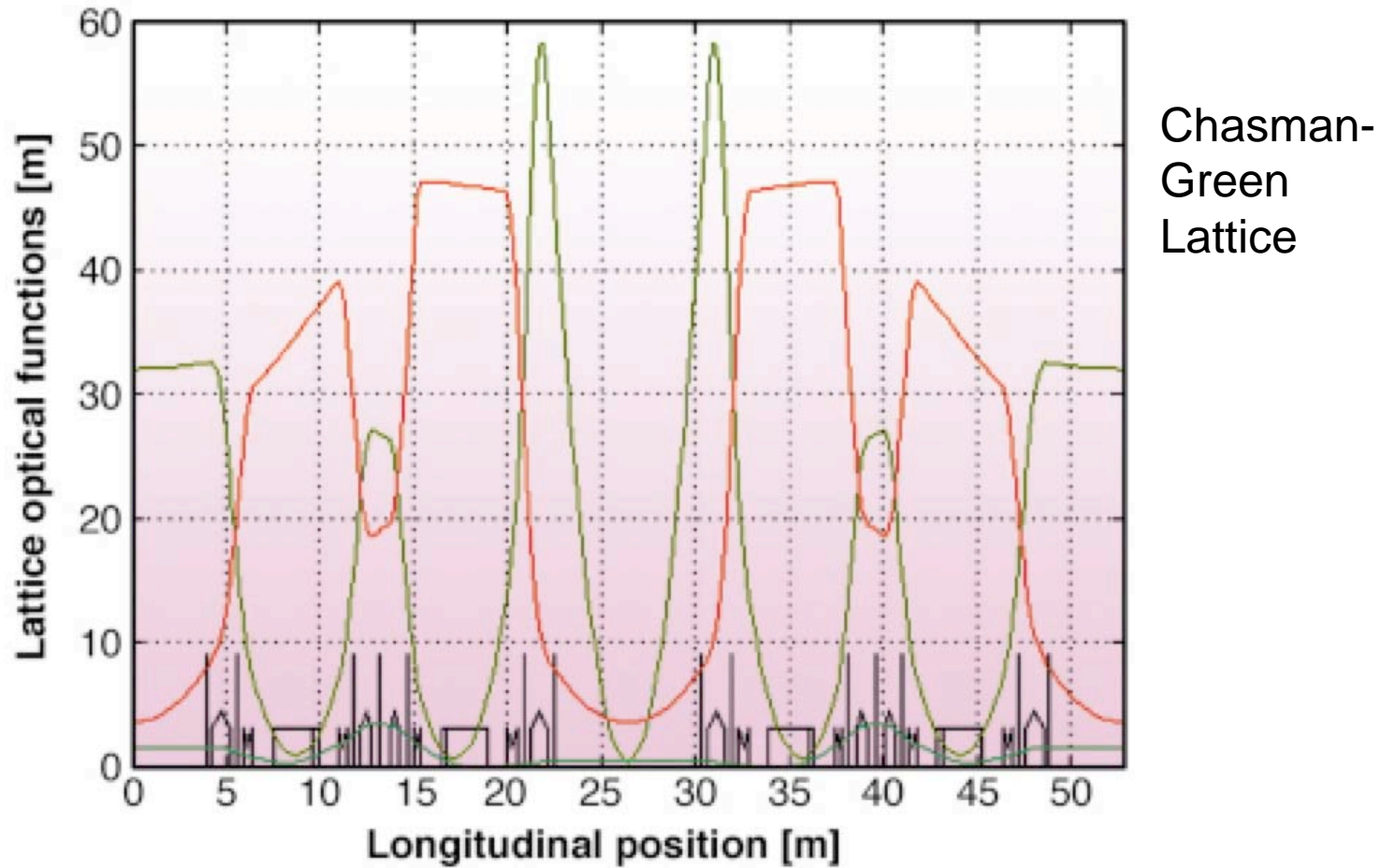
Gamma - ray energy resolution in the linear theory (with correlations):

$$\sigma_k \cong \frac{E \sigma_{xT}}{d} \approx 6.9 \text{ MeV for Graal (FWHM} = 16 \text{ MeV)}$$

$$\sigma_{xT}^2 \cong \varepsilon_x \beta_{xT} + \eta_T^2 \sigma_p^2 \quad \text{at the position of the Tagger}$$

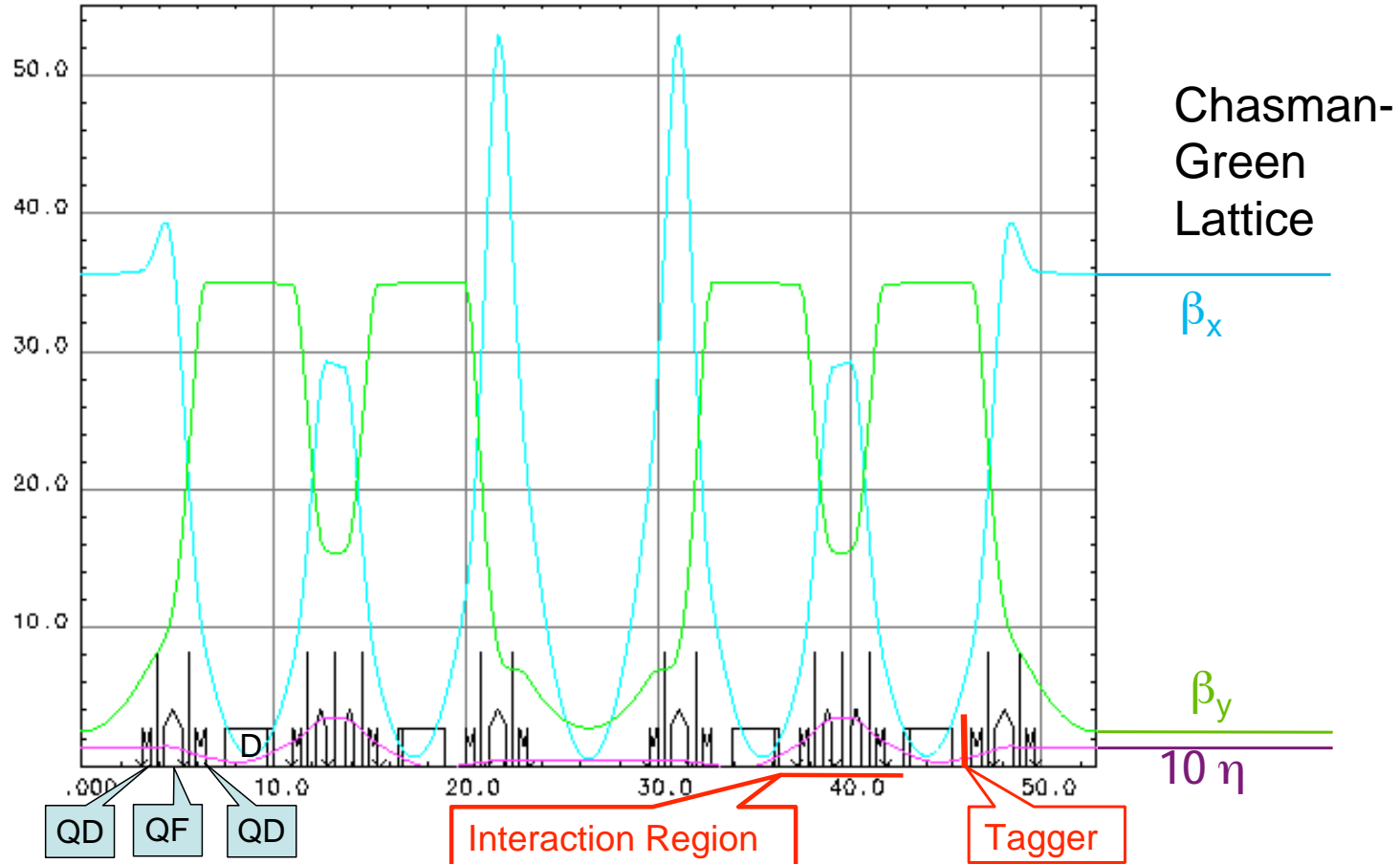
E	Electron beam energy (MeV) (6.03 GeV)
σ_k	Gamma-ray energy resolution (MeV)
σ_E	Energy spread of the stored electron beam = $E \sigma_p$ ($\cong 6030 \cdot 0.0011 \cong 6.6$ MeV)
$\sigma_{E'}$	Energy resolution of the electron tagging system (MeV)
σ_{xT}	Horizontal dispersion of the electron beam at the tagger (m)
d	Dispersion of the ring magnets from the interaction point to the tagger position (m)
ε_x	Horizontal emittance of the electron beam ($\cong 4$ nm)
β_{xt}	Horizontal betatron wave length at the tagger (m)
η_T	Spatial energy dispersion of the electron beam at the tagger (m)
σ_p	Fractional energy dispersion of the electron beam (0.11%)

The ESRF Magnetic Lattice Structure: NOW



The ESRF Magnetic Lattice Structure: ORIGINAL

NUX = 36.440 R = 134.3889
 NUZ = 14.391 ALPHA= 1.683E-04 OPTICAL FUNCTIONS Ex/Gam+*2= 2.713E-17



The ESRF Magnetic Lattice Structure: ORIGINAL

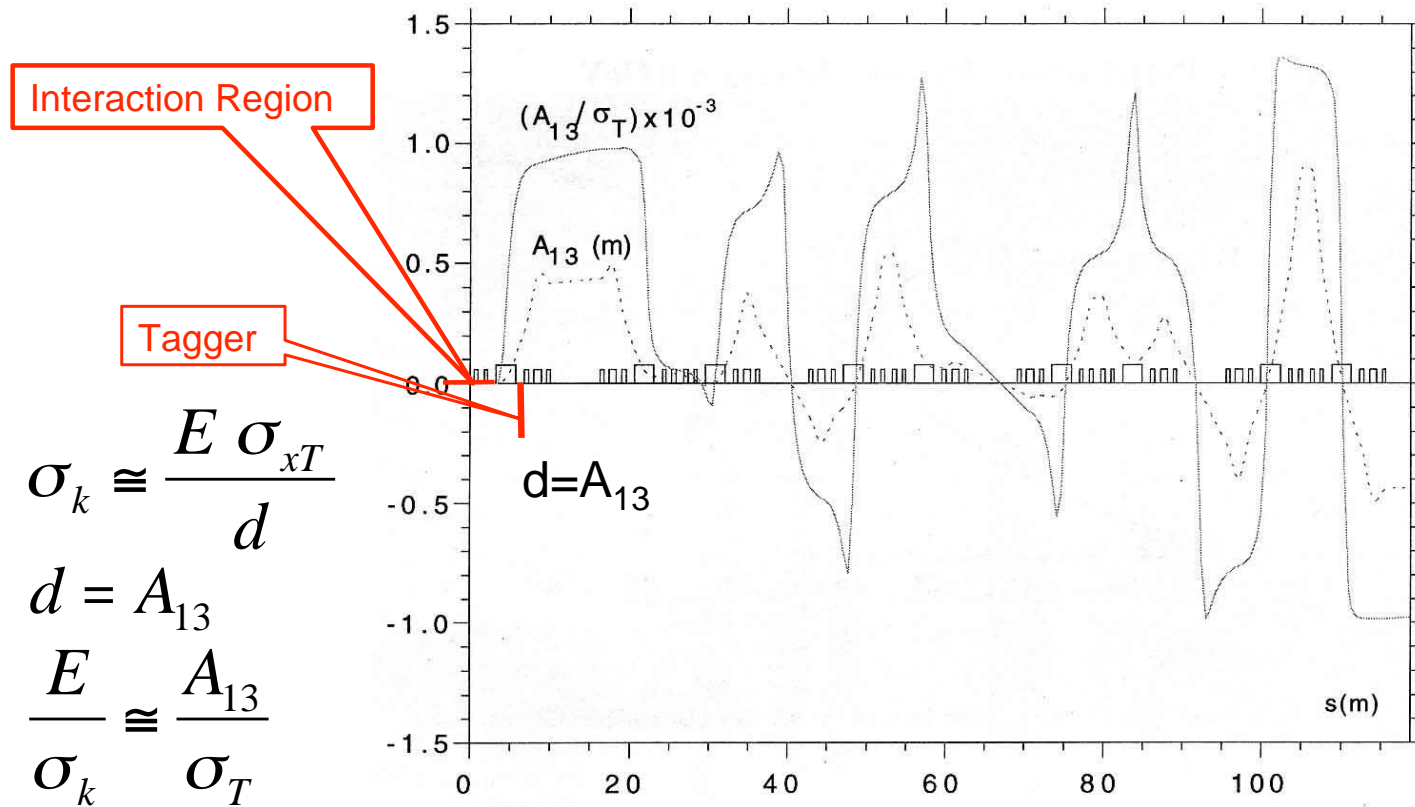
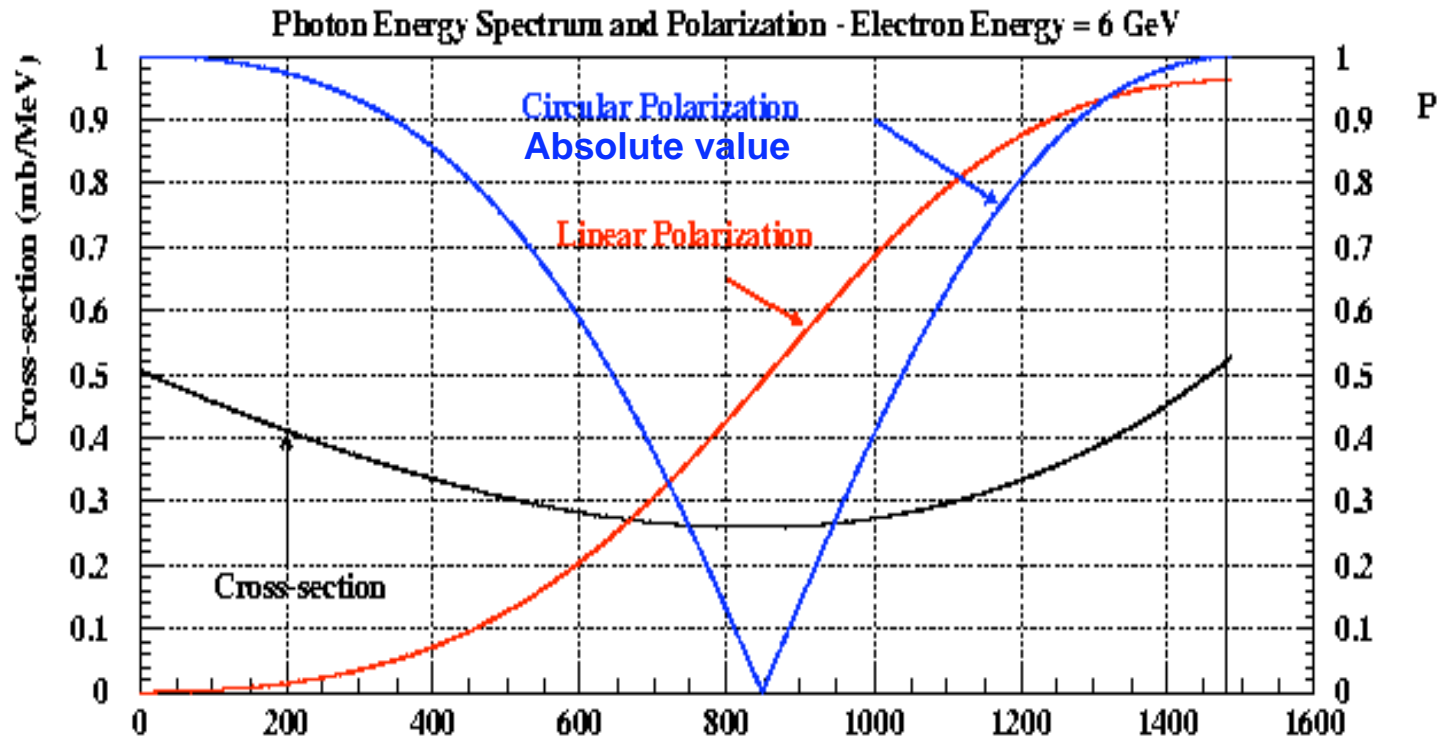


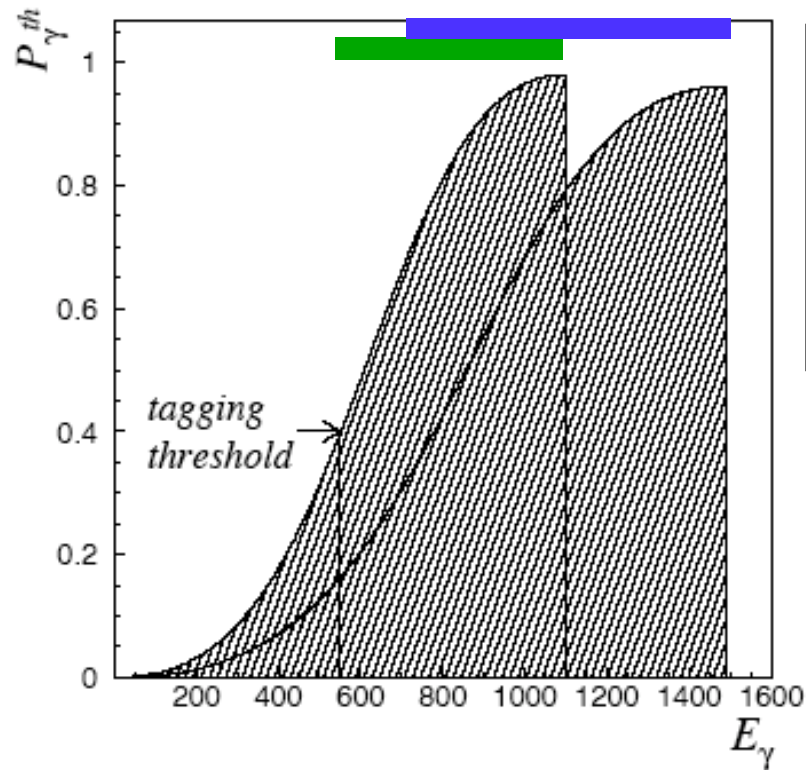
Figure 14 – Dispersion and energy resolution at the ESRF as a function of the position of the tagger, calculated from the centre of a short straight section.

Graal Beam Polarization

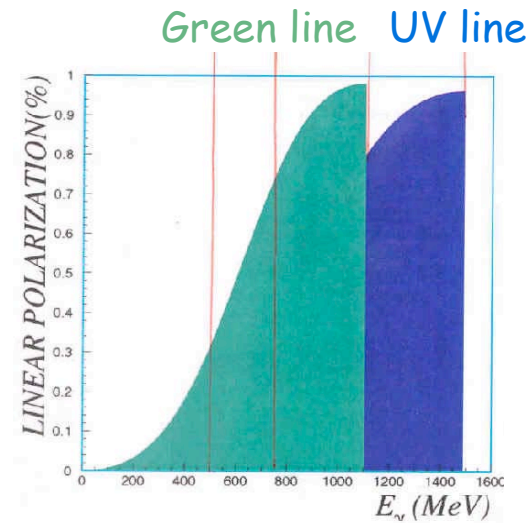


The shape of the cross section produces a flat spectrum

Graal Beam Polarization: Green vs UV

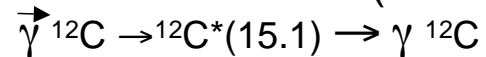


Theoretical linear polarization of the γ -ray beam for two laser lines: $\lambda = 514$ nm (green line) and $\lambda = 351$ nm (UV line). The threshold energy of the tagging system is also shown

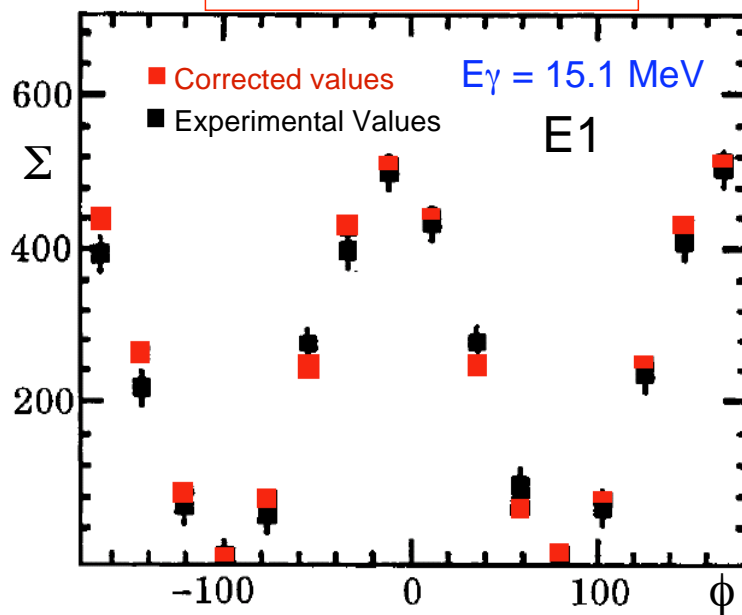


$\vec{\gamma}$ Beam Polarization Measurements ^{12}C

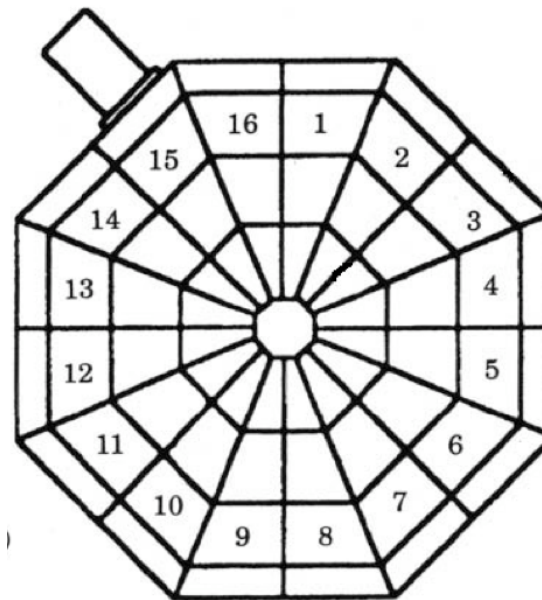
Ladon – Frascati (1975)



$$\langle P \rangle = 0.99 \pm 0.02$$

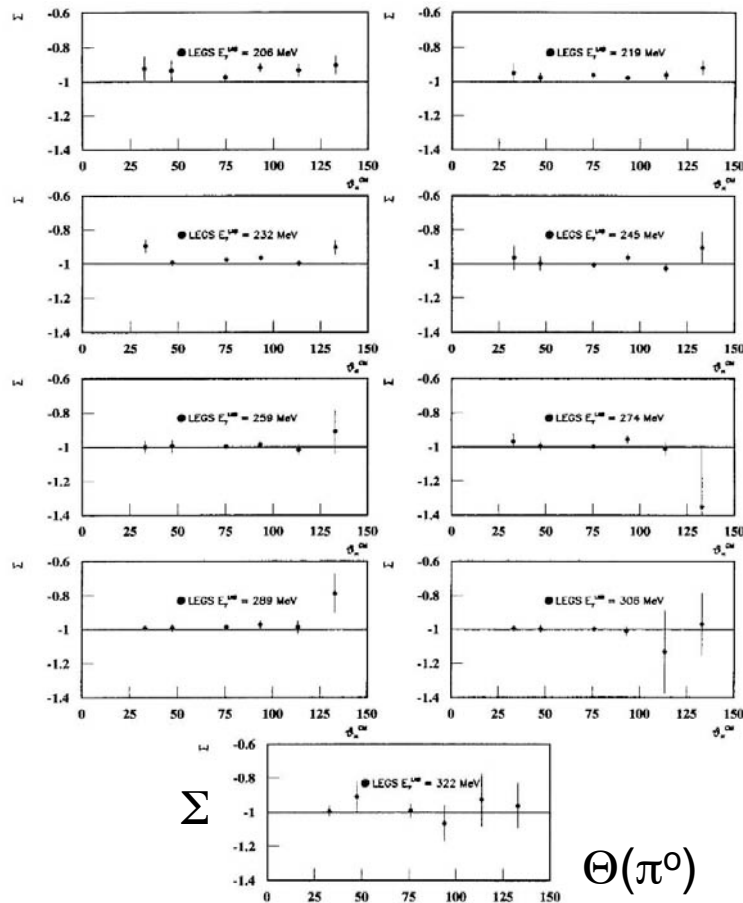


$(1 + \cos 2\phi)$ distribution at $\theta = 90^\circ$



Small NaI crystal ball ($7_\theta \times 16_\phi$) of the University of Rome "La Sapienza"

$\vec{\gamma}$ Beam Polarization Measurements ${}^4\text{He } \pi^0$ LEGS - BNL 2003



$\vec{\gamma} {}^4\text{He} \rightarrow \pi^0 {}^4\text{He}$ (coherent)

$E_\gamma = 200\text{-}322 \text{ MeV}$ M1

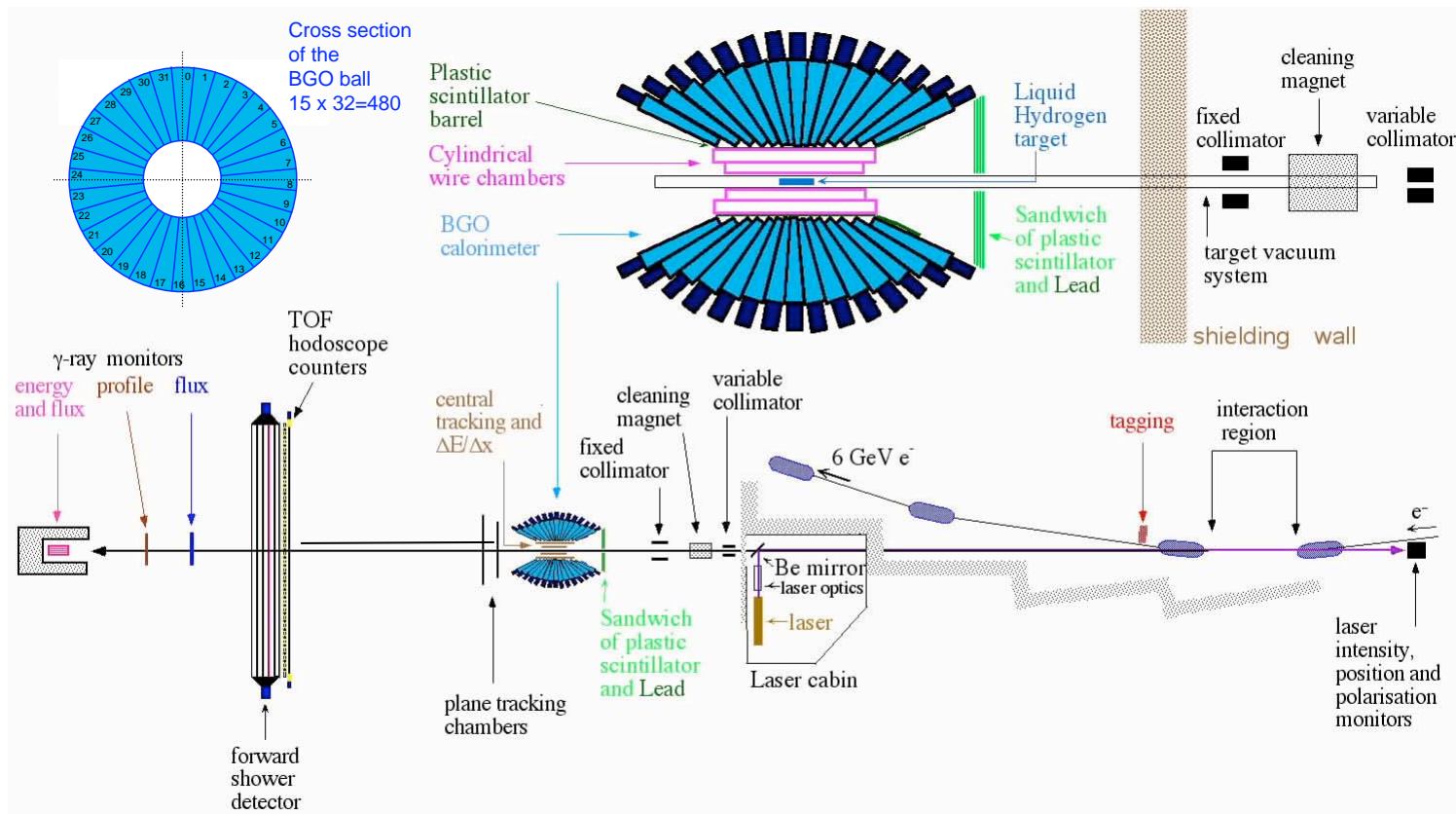
Since the π^0 is a pseudoscalar (spin=0), and also ${}^4\text{He}$ has spin 0, the only pseudoscalar that can be formed with the available kinematical vectors ($\vec{k}_\gamma, \vec{\varepsilon}_\gamma, \vec{q}_\pi$) is the triple vector product \mathbf{A} .

$$\mathbf{A} = \vec{k}_\gamma \cdot \vec{\varepsilon}_\gamma \times \vec{q}_\pi \quad \Sigma = -1$$

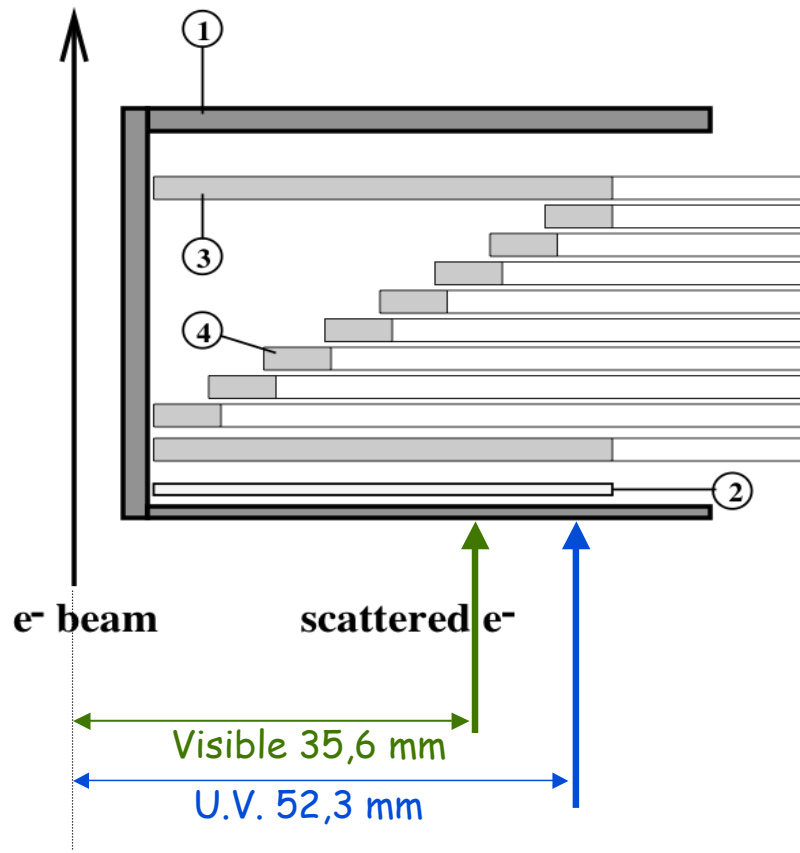
\vec{k}_γ is the photon momentum,
 $\vec{\varepsilon}_\gamma$ is the photon linear polarization vector
 \vec{q}_π is the momentum of the π^0

$$\langle P \rangle = 0.98 \pm 0.02$$

The Graal Apparatus



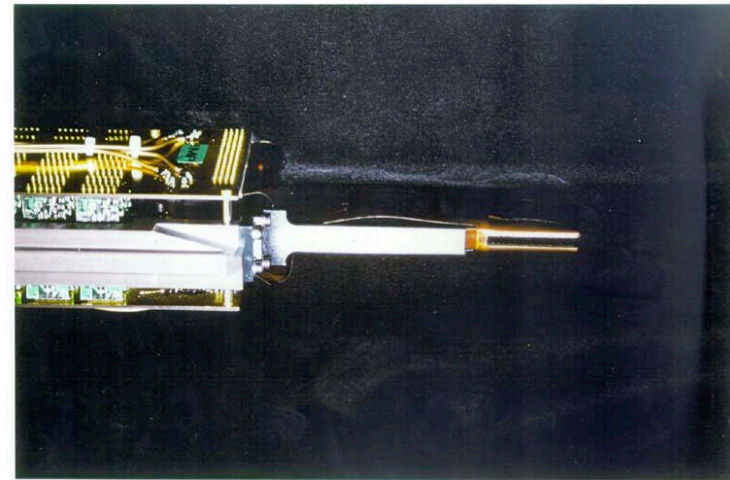
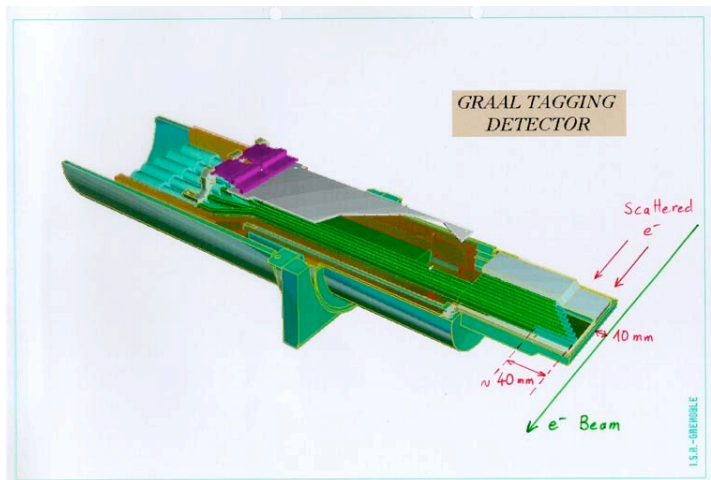
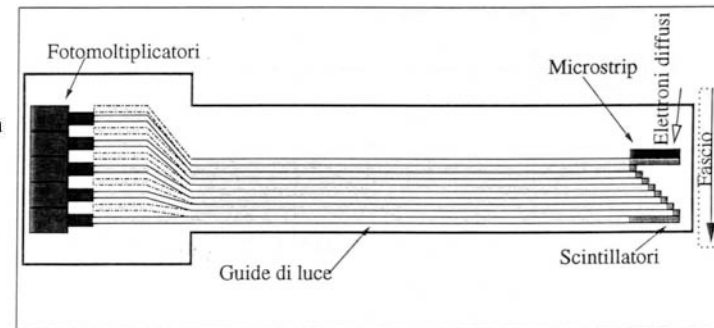
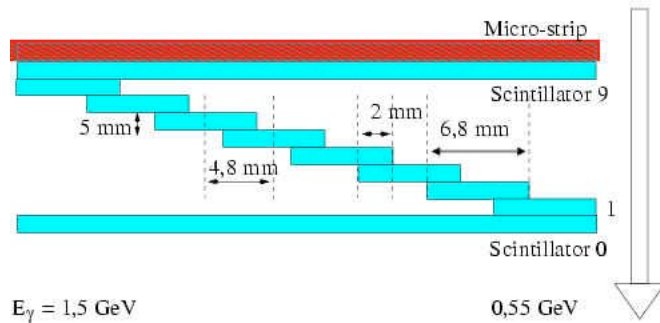
Graal Tagging Detector



- 1 : Shielding 4 mm
- 2 : 128 Si Microstrips
Pitch = 300 μm
Length = 38,4 mm
- 3-4 : Scintillators

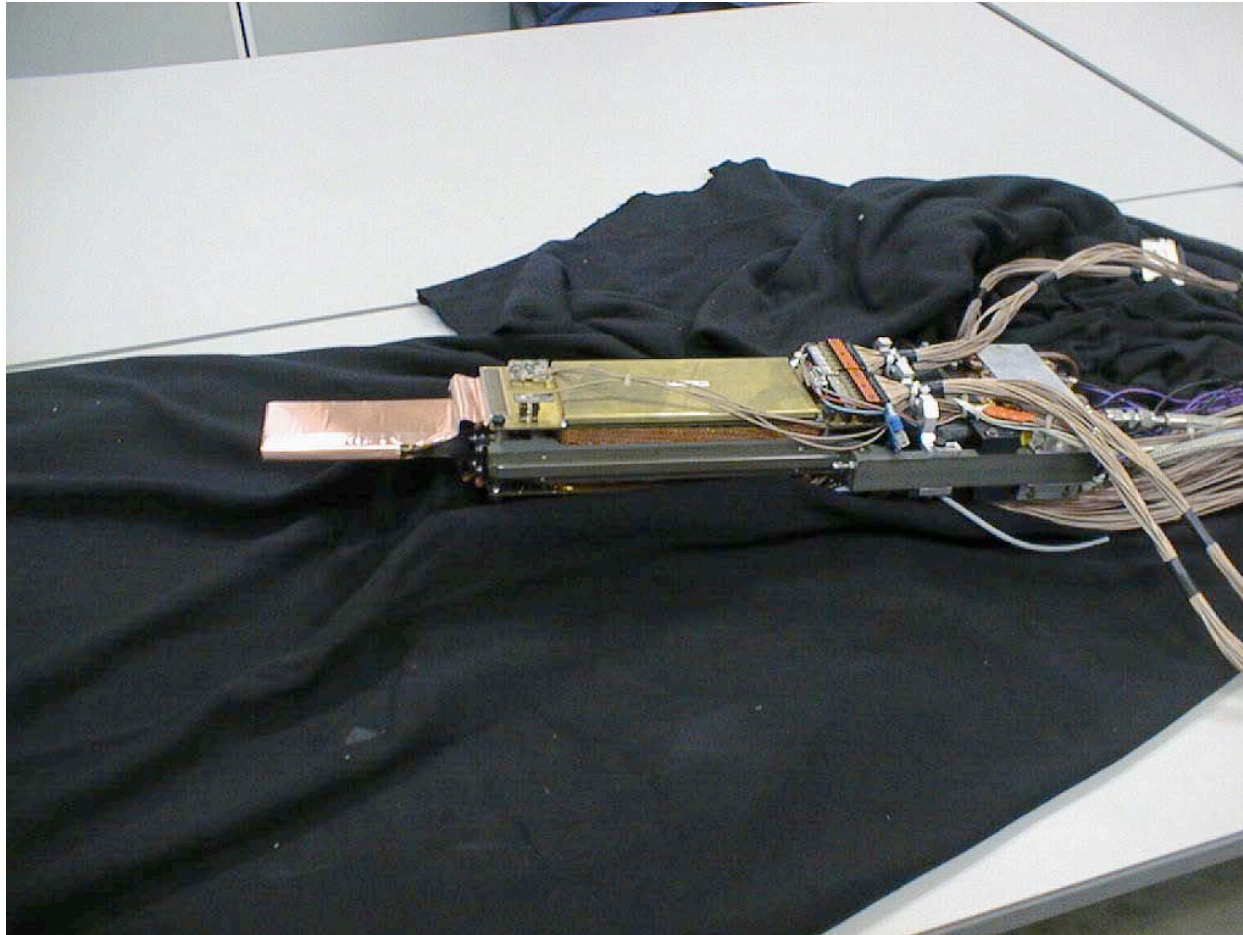
NOT IN SCALE

The Graal Tagging Detector



128 μ strip silicon detector + 10 fast plastic scintillators, located inside the storage ring behind the first dipole after the interaction region

The Tagging Detectors

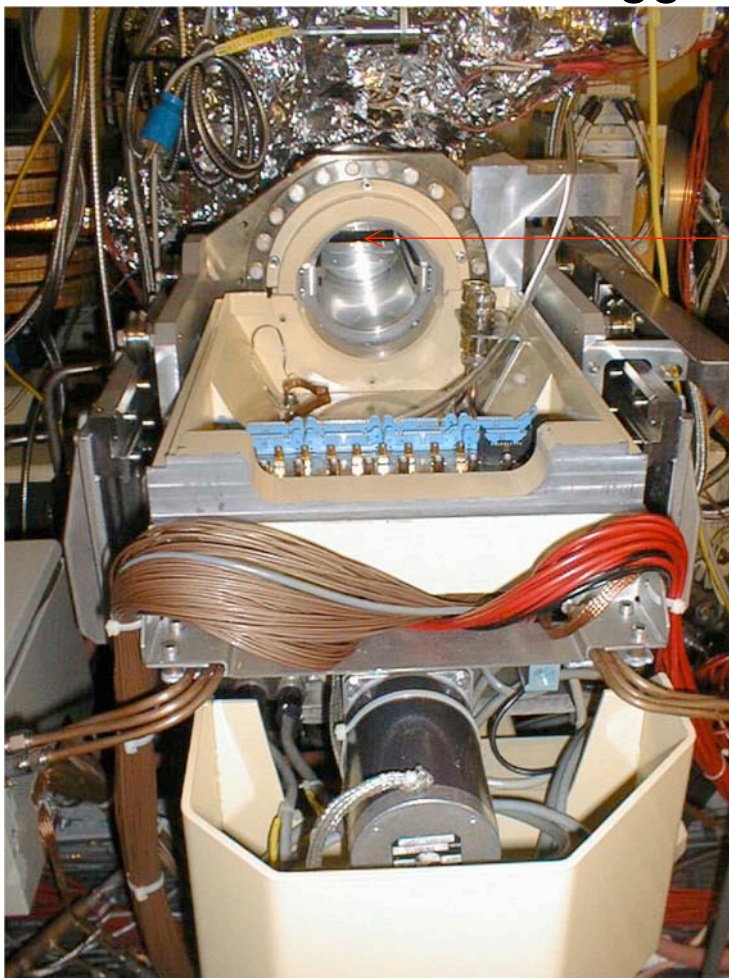


6/26/09

Carlo Schaerf Yerevan 1/06/09

25

The Tagger Container



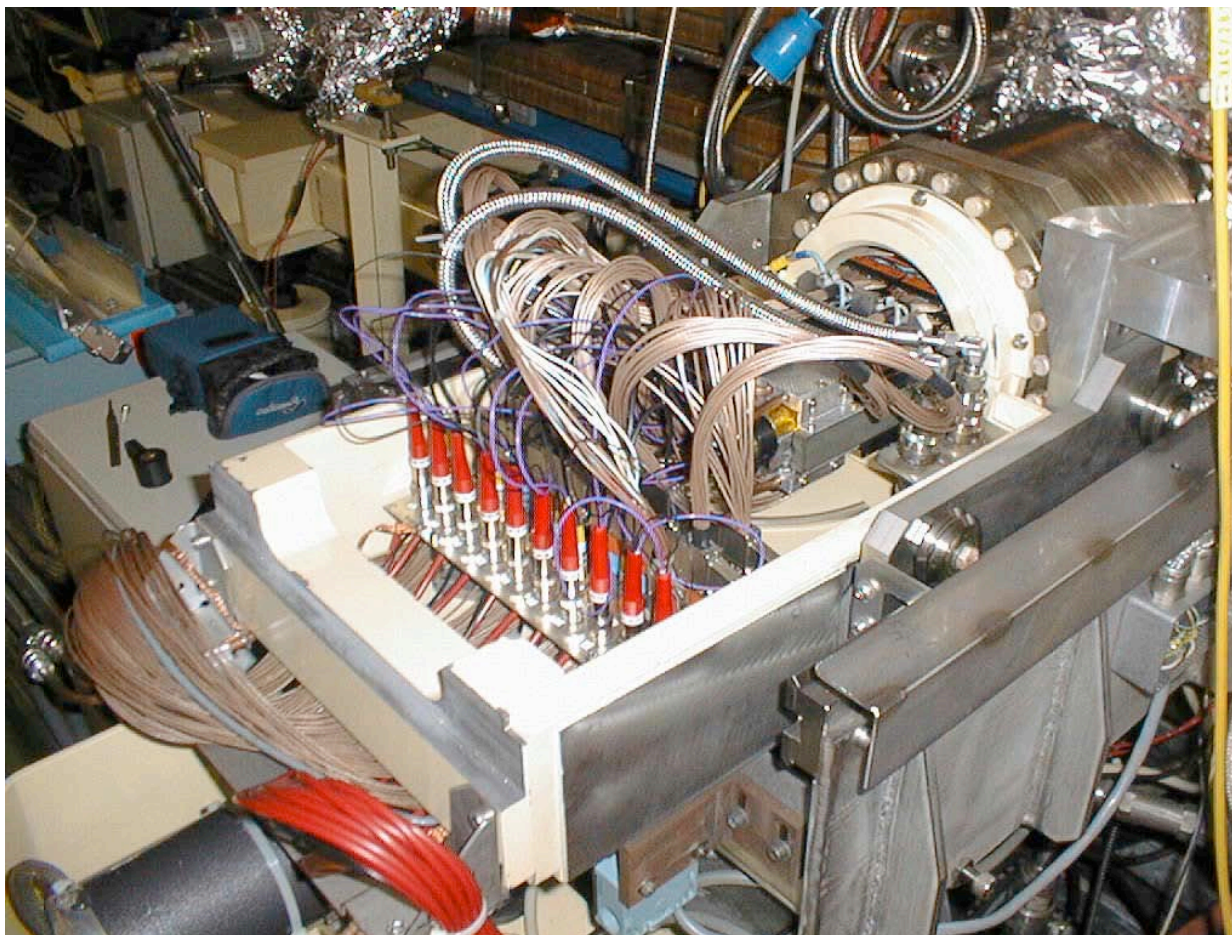
The detector fits in here

6/26/09

Carlo Schaerf Yerevan 1/06/09

26

The Tagger Connections



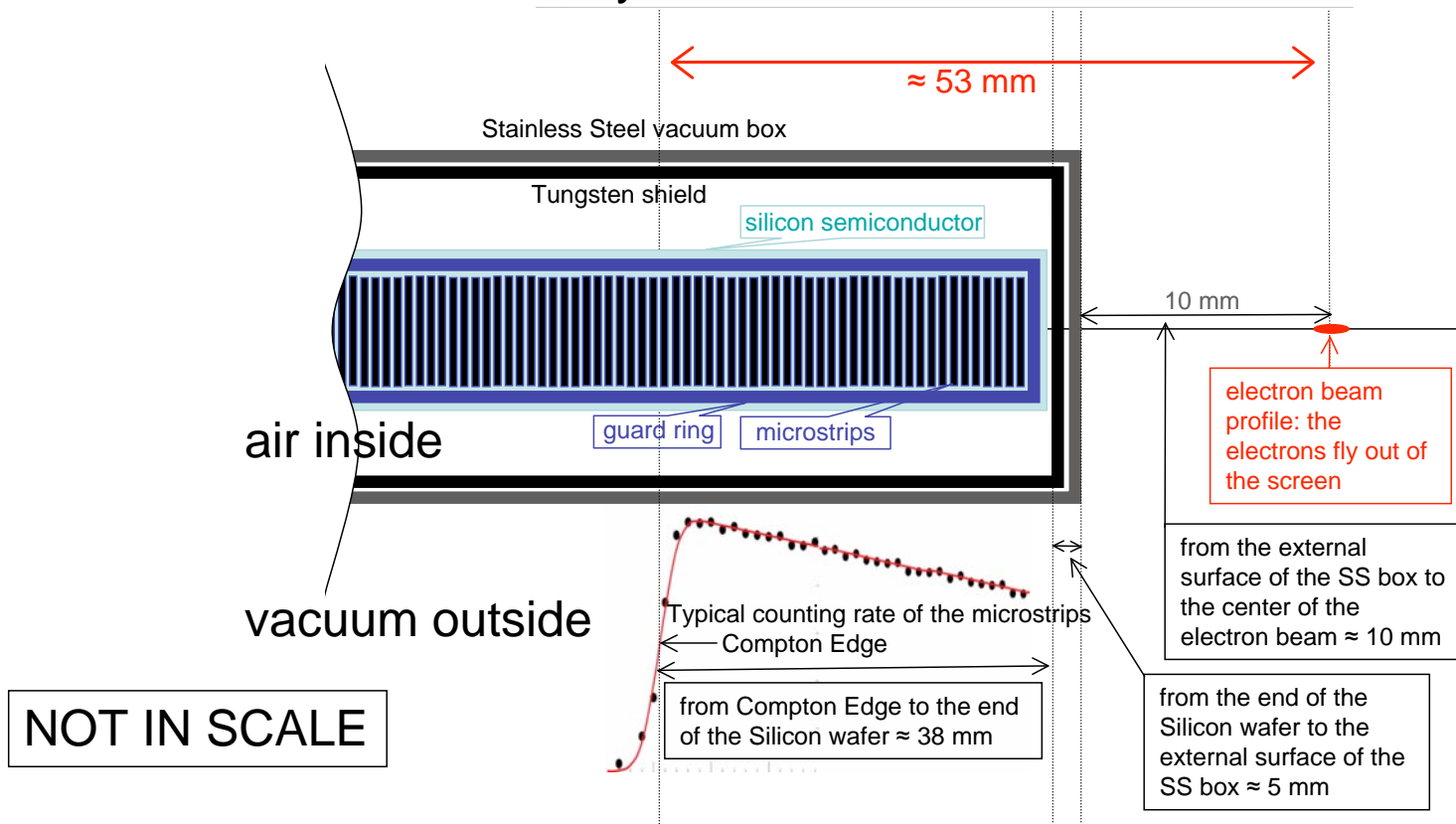
6/26/09

Carlo Schaerf Yerevan 1/06/09

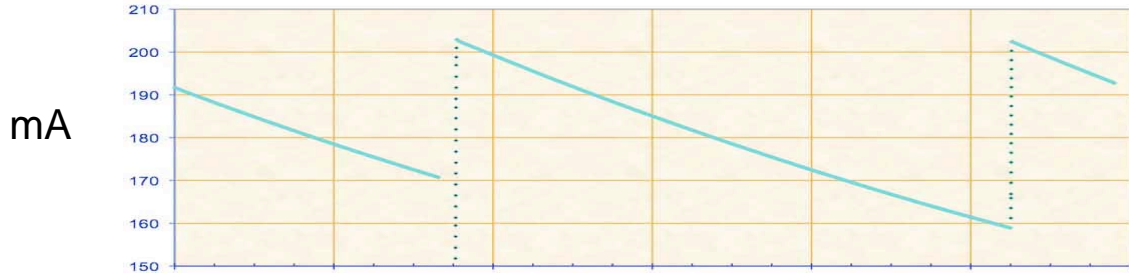
27

Graal Tagging Microstrips

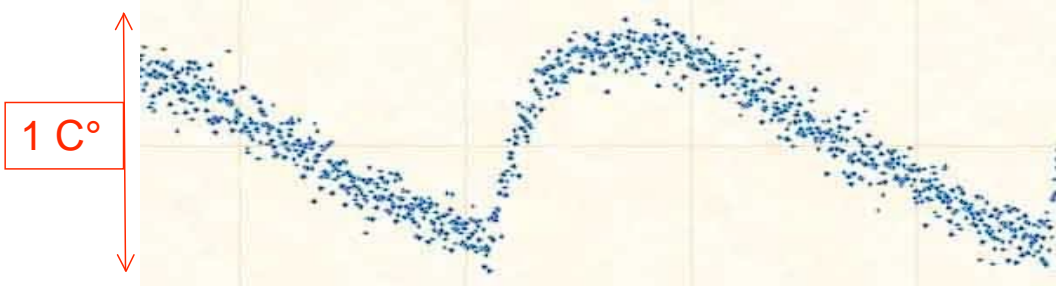
Schematic description of the tagging detector in more details.
Vertical cut: the electrons fly out of the screen.



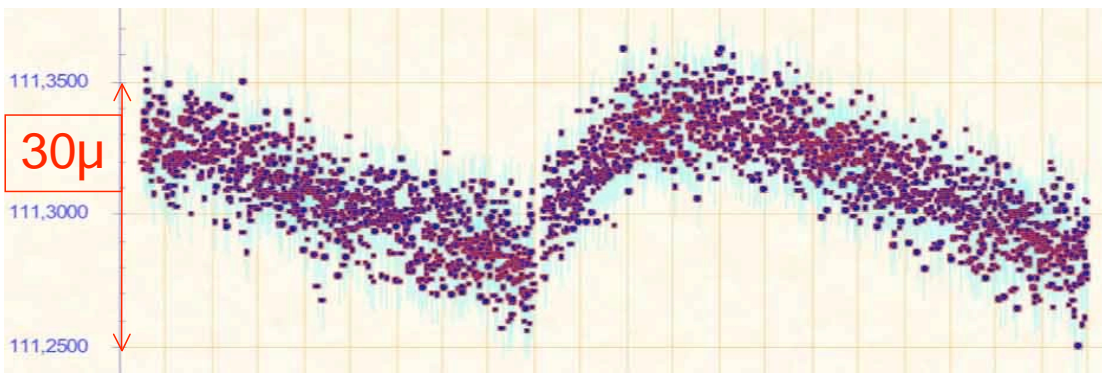
Temperature in the Tagging Box



Electron current in the ESRF
mA



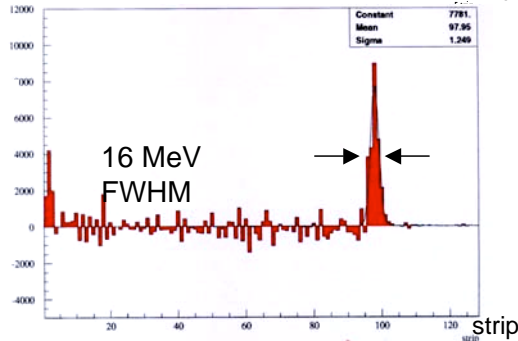
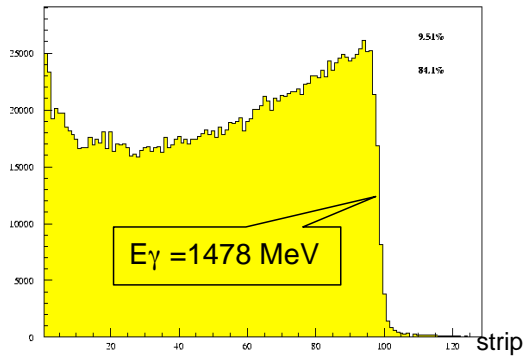
Temperature in the tagging box
C°



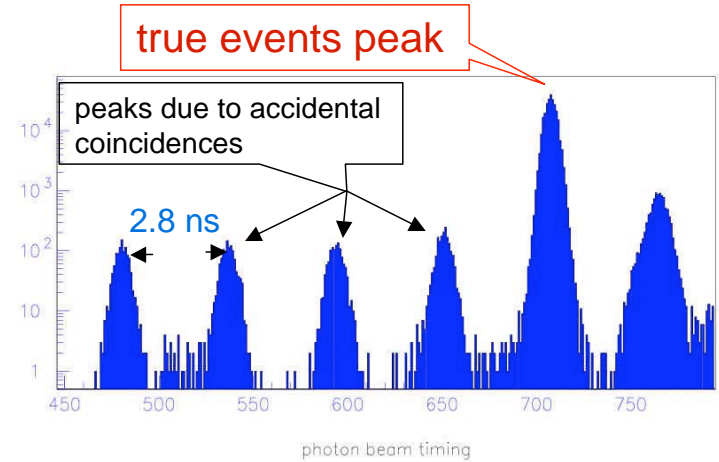
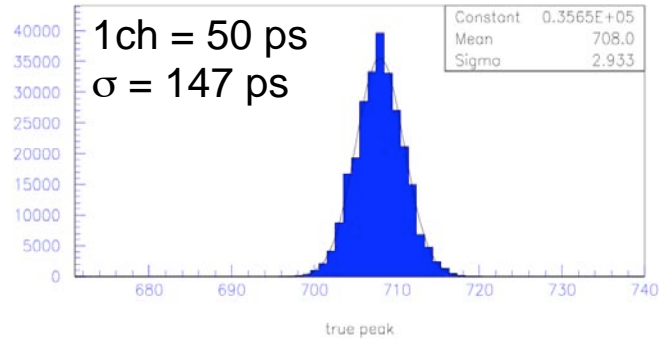
Position of the Compton Edge
1 microstrip = 300 μm

Energy and timing resolution 1 UV line

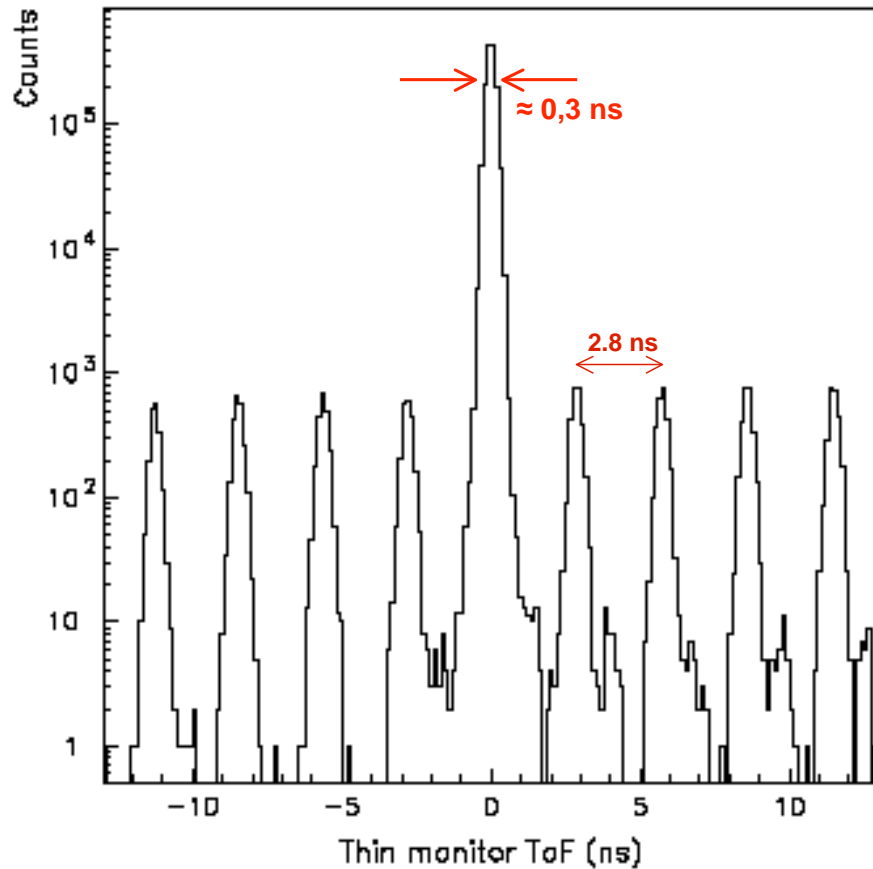
The energy resolution provided by the internal tagging technique:
 μ-strip silicon detector → energy resolution of 16 MeV (FWHM) (1.1%)
 plastic scintillators → time resolution better than 500 ps (FWHM)



Tagged spectrum

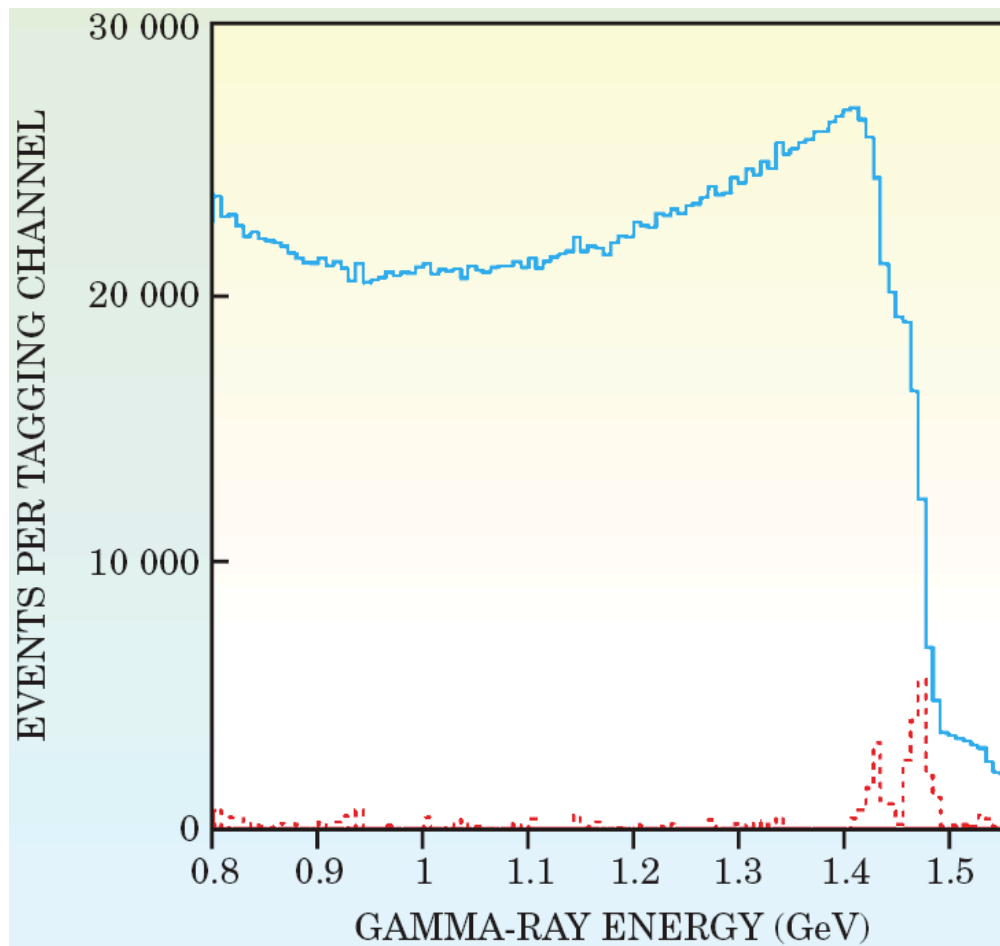


Time Of Flight resolution



Typical experimental Time Of Flight spectrum for the thin monitor versus the tagging counters. The distance between two adjacent peaks is 2.8 ns corresponding to the distance between successive electron bunches. The timing resolution is ≈ 0.3 ns (FWHM). The level of accidental coincidences in the main peak is less than 0.15%.

Gamma-ray Energy Spectrum - 3 UV lines



Graal beam with
3 UV laser lines

Compton Scattering Kinematics 1/3

2. The maximum energy lost by the electrons after an elastic scattering with a laser photon is given by the maximum energy acquired by the photon:

$$E_{el}^0 - E_{el}^{scatt} = E_{\gamma \max} = \frac{4\gamma^2 E_{laser}}{1 + \frac{4\gamma E_{laser}}{m_e}} \approx 4\gamma^2 E_{laser}$$

This energy loss is measured by the displacement \mathbf{d} of the scattered electrons from the primary electron beam after the first magnetic dipole. For the ESRF electron energy of 6.03 GeV and a UV laser line of 3.53 eV, the energy loss is 1.487 GeV and corresponds to an electron displacement at the position of the Graal tagging detector: $\mathbf{d} \approx 52.3$ mm.

The microstrips of the Graal tagging detector measure the displacement \mathbf{d} of the scattered electrons from the main orbit and therefore the energy lost by the electrons (and acquired by the gamma-rays):

$$E_{\gamma} \propto d$$

Compton Scattering Kinematics 2/3

3. From the relativistic kinematics of Compton scattering:

$$E_{\gamma \max} = \frac{4\gamma^2 E_{laser}}{1 + \frac{4\gamma E_{laser}}{m_e}} \approx 4\gamma^2 E_{laser} \quad \text{and} \quad \frac{dE_\gamma}{E_\gamma} \approx 2 \frac{d\gamma}{\gamma} \quad \text{or} \quad \frac{d\gamma}{\gamma} \approx \frac{1}{2} \frac{dE_\gamma}{E_\gamma}$$

and in general from relativistic kinematics:

$$\beta d\beta = \left(\frac{1}{\gamma^2} \right) \frac{d\gamma}{\gamma} \approx \frac{1}{2} \left(\frac{1}{\gamma^2} \right) \frac{dE_\gamma}{E_\gamma} \quad \text{or} \quad \Delta\beta \approx \frac{1}{2} \left(\frac{1}{\gamma^2} \right) \frac{\Delta E_\gamma}{E_\gamma}$$

since at the ESRF:

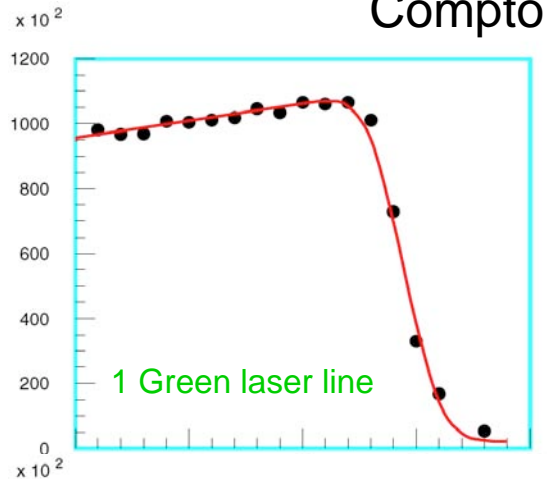
$$\gamma = \frac{E_e}{m_e} = \frac{6030}{0.511} = 11\,800; \quad 2\gamma^2 \approx 2.8 \cdot 10^8$$

we have:

$$\Delta\beta \approx \frac{1}{2} \left(\frac{1}{\gamma^2} \right) \frac{\Delta E_\gamma}{E_\gamma} \approx \frac{1}{2.8 \cdot 10^8} \cdot \frac{\Delta E_\gamma}{E_\gamma} \approx 0.4 \cdot 10^{-8} \frac{\Delta E_\gamma}{E_\gamma} \approx 0.4 \cdot 10^{-8} \frac{\Delta d}{d}$$

The error in β is reduced by eight orders of magnitude with respect to the relative error in d (the displacement of the scattered electrons from the main orbit).

Compton Scattering Kinematics 3/3



$$E_{\gamma \max} = \frac{4\gamma^2 E_{\text{laser}}}{1 + \frac{4\gamma E_{\text{laser}}}{m_e}} \approx 4\gamma^2 E_{\text{laser}}$$

$$\frac{dE_{\gamma}}{E_{\gamma}} \approx 2 \frac{d\gamma}{\gamma}; \quad \beta d\beta = \left(\frac{1}{\gamma^2} \right) \frac{d\gamma}{\gamma}$$

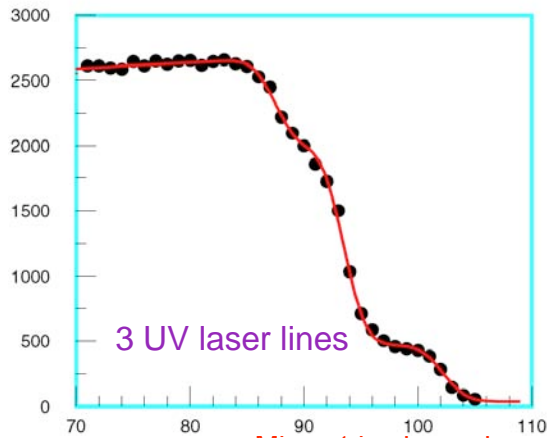
$$\gamma = \frac{E_e}{m_e} = \frac{6030}{0.511} = 11\,800; \quad \gamma^2 \approx 1.4 \cdot 10^8$$

A typical accuracy of 0.03 microstrip (= 9 μ) is obtained for the position of a given line, corresponding to 0.2 MeV.

$$\frac{\Delta E_{\gamma}}{E_{\gamma}} \approx 2 \cdot 10^{-4}; \quad \frac{\Delta\gamma}{\gamma} \approx \frac{1}{2} \frac{\Delta E_{\gamma}}{E_{\gamma}} \approx 10^{-4}$$

$$\Delta\beta = \left(\frac{1}{\gamma^2} \right) \frac{\Delta\gamma}{\gamma} \approx 10^{-8} \cdot 10^{-4} \approx 10^{-12}$$

Published: < 3 · 10⁻¹²



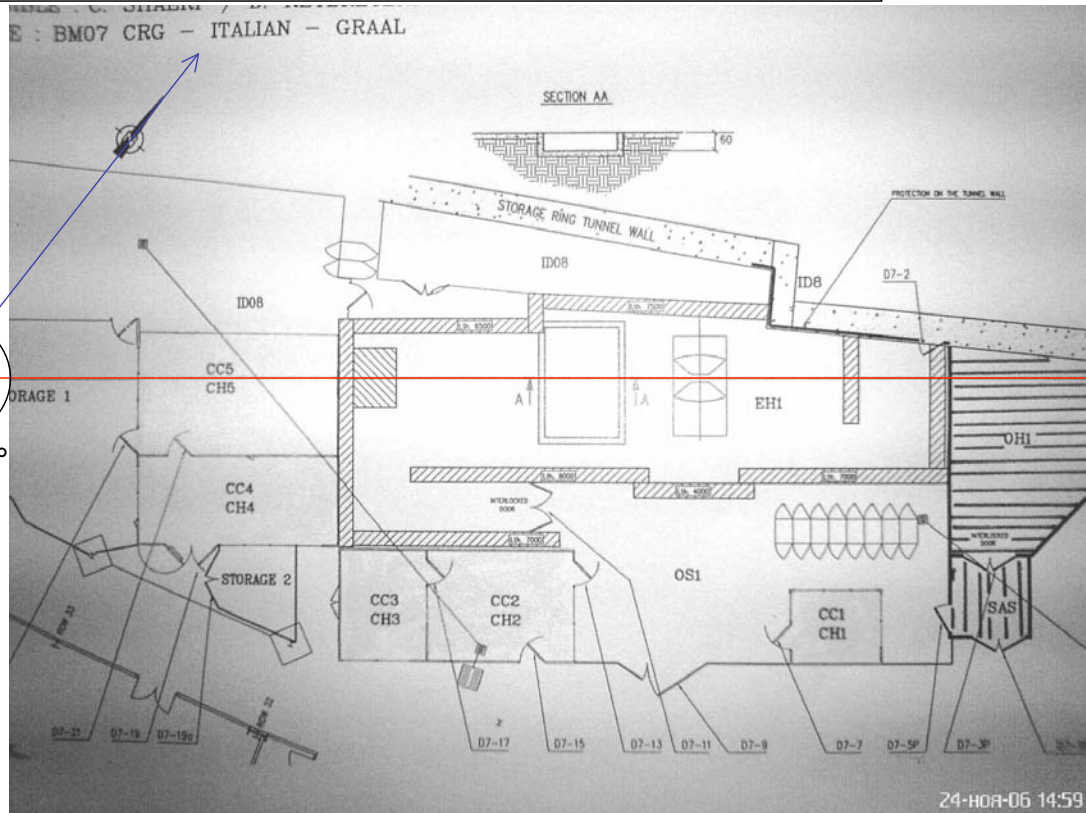
Microstrip channels
1 channel = 0.3 mm \approx 6.6 MeV

Graal Beam Orientation on the Earth

The Graal beam points approximately to the S-W

≈S-W
(225°)

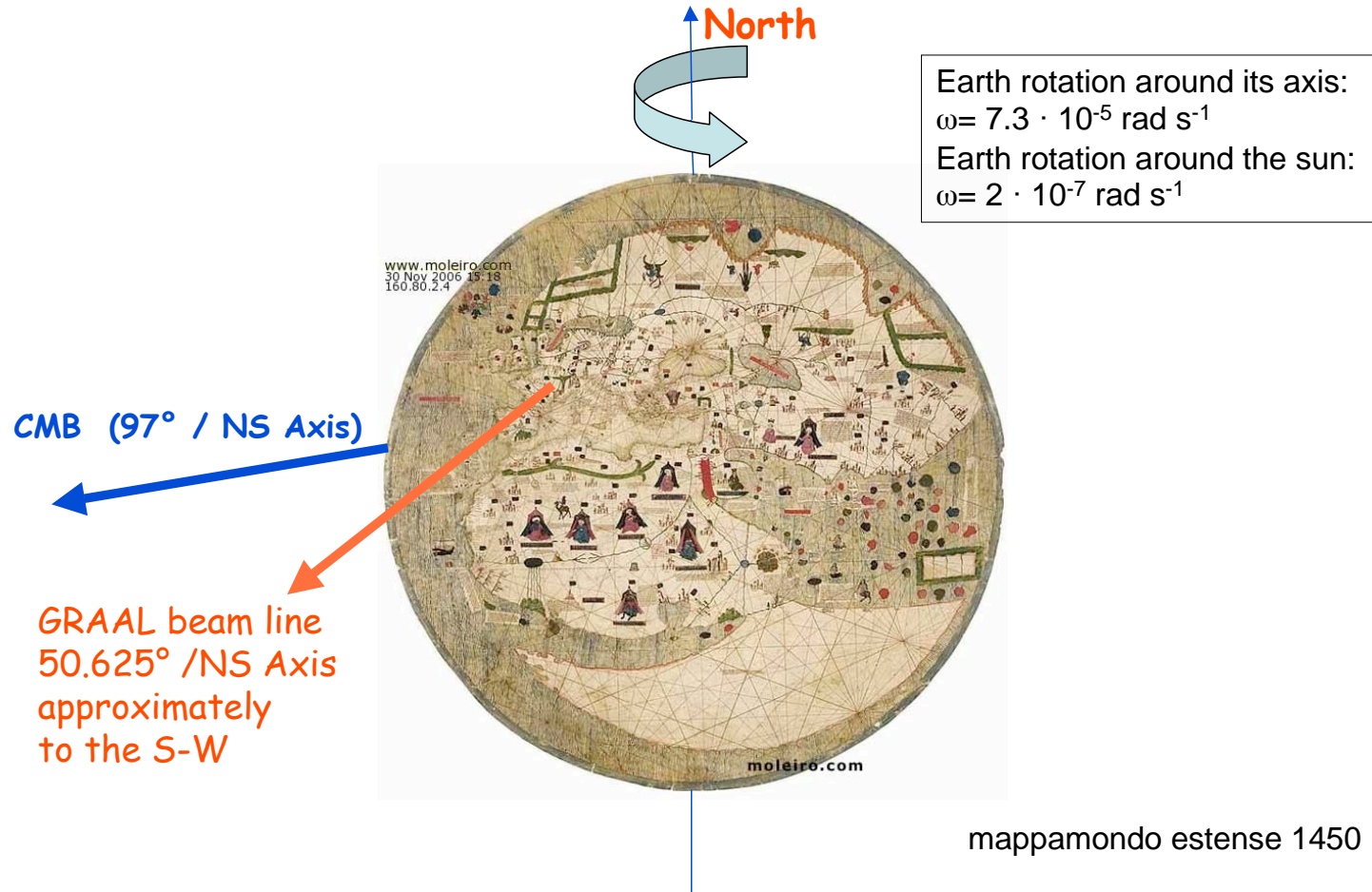
230.6°



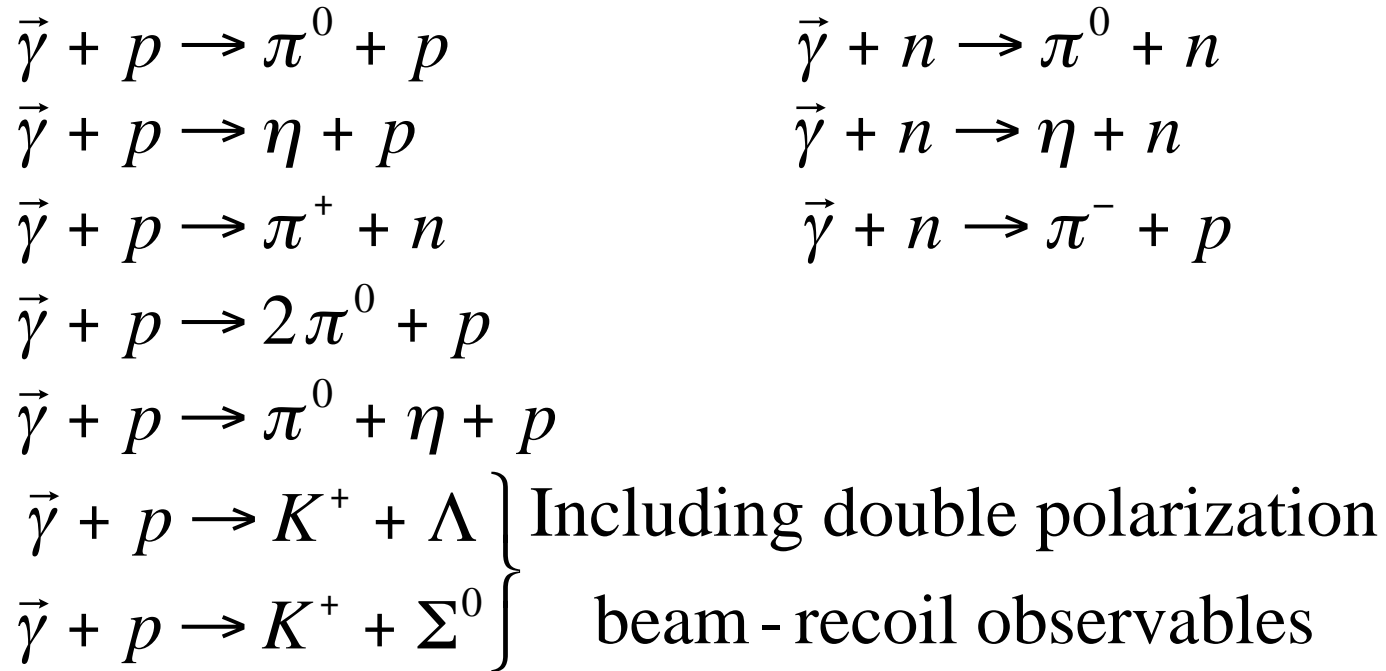
Earth rotation around its axis: $\omega = 7.3 \cdot 10^{-5} \text{ rad s}^{-1}$

Earth rotation around the sun: $\omega = 2 \cdot 10^{-7} \text{ rad s}^{-1}$

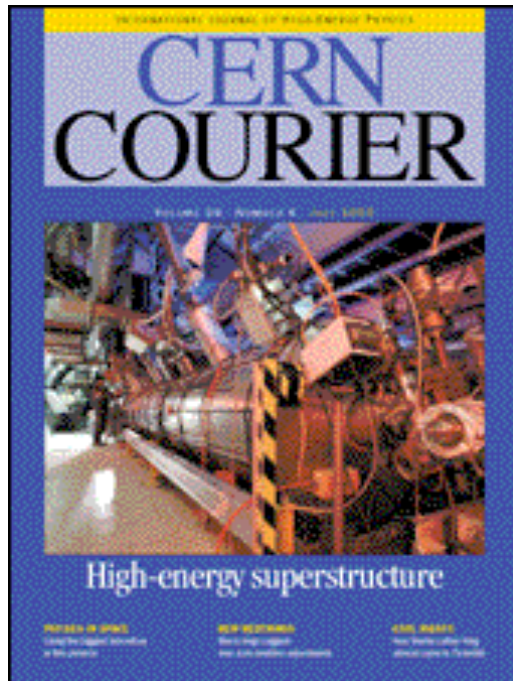
Graal Rotations and the CMB



The Graal Experimental Program



CERN Courier 1999



28 Jun 1999

INTERNATIONAL JOURNAL OF HIGH-ENERGY PHYSICS



Photon beams

The Graal of particle physics

A new particle physics experiment uses a very different setting : the European Synchrotron Radiation Facility electron ring in Grenoble.

Physics Today 2005

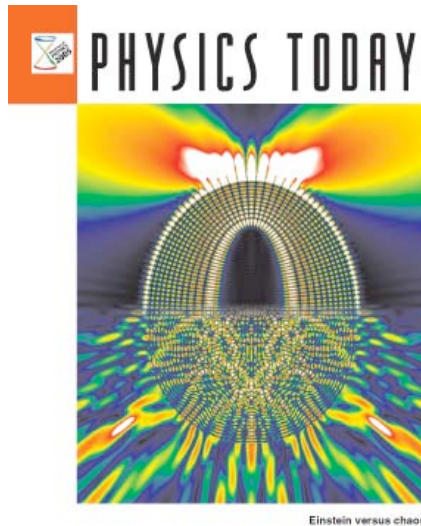


Table of Contents August 2005

Features

Pyroelectricity: From Ancient Curiosity to Modern Imaging Tool

Changes in the net dipole moment of certain materials form the basis for a broad range of IR detectors — *Sidney B. Lang*

Einstein's Unknown Insight and the Problem of Quantizing Chaos

Chaotic systems were beyond the reach of an ingenious coordinate-invariant quantization scheme developed by Albert Einstein, and to this day, their quantization remains a challenge — *A. Douglas Stone*

Polarized Gamma-Ray Beams

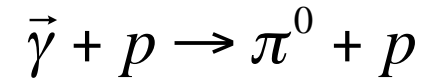
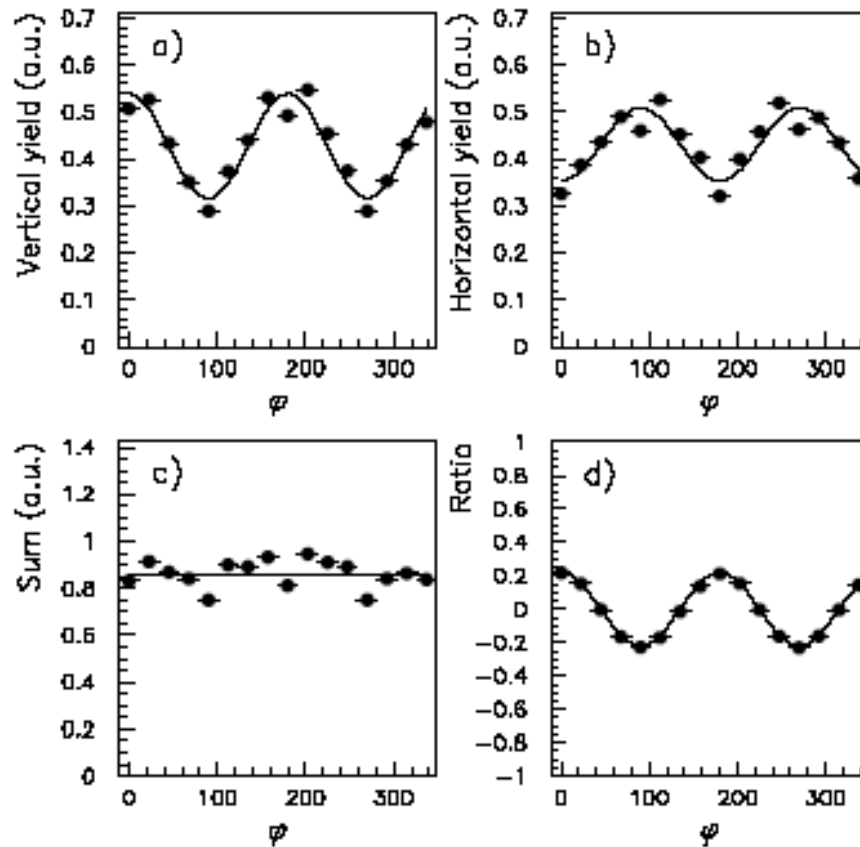
Polarized high-energy photons are excellent probes of protons, neutrons, and nuclei. Nowadays they are readily made by shining laser light at a high-energy electron beam. — *Carlo Schaerf*



Polarized Gamma-Ray Beams

Polarized high-energy photons are excellent probes of protons, neutrons, and nuclei. Nowadays they are readily made by shining laser light at a high-energy electron beam.
— *Carlo Schaerf*

The azimuthal distribution in φ

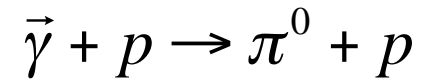
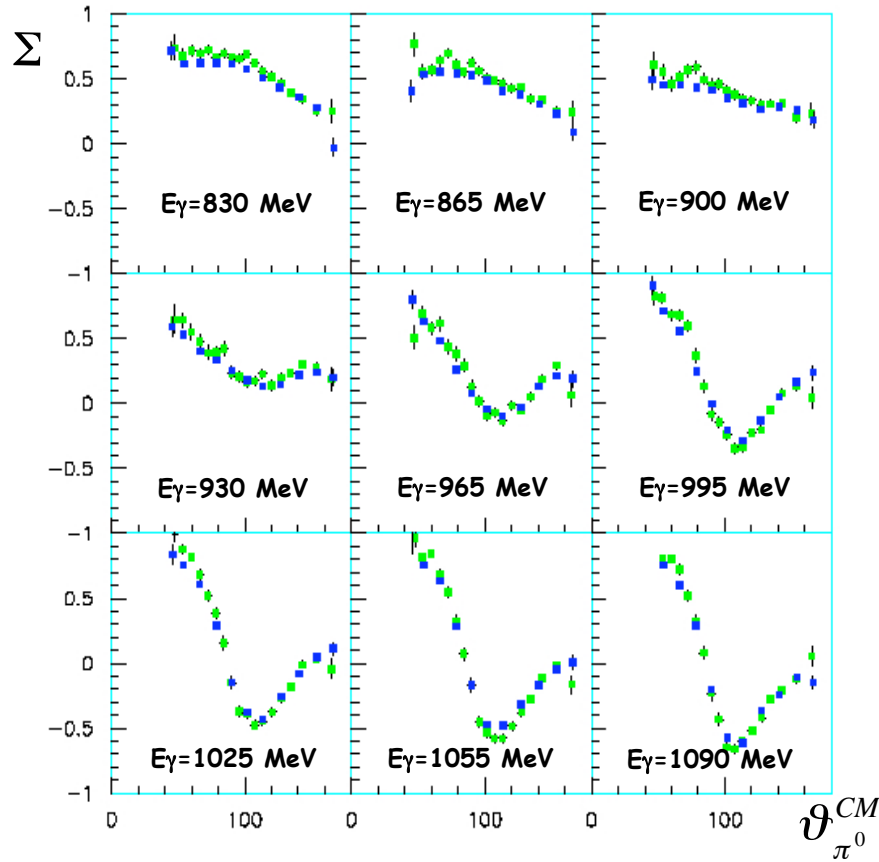


Yields as a function of φ
 for one value of θ and E_γ :
 a) Vertical polarization;
 b) Horizontal polarization;
 c) Sum of a and b;
 d) The ratio (a-b)/(a+b)

The solid line in d presents
 a fit of the type:

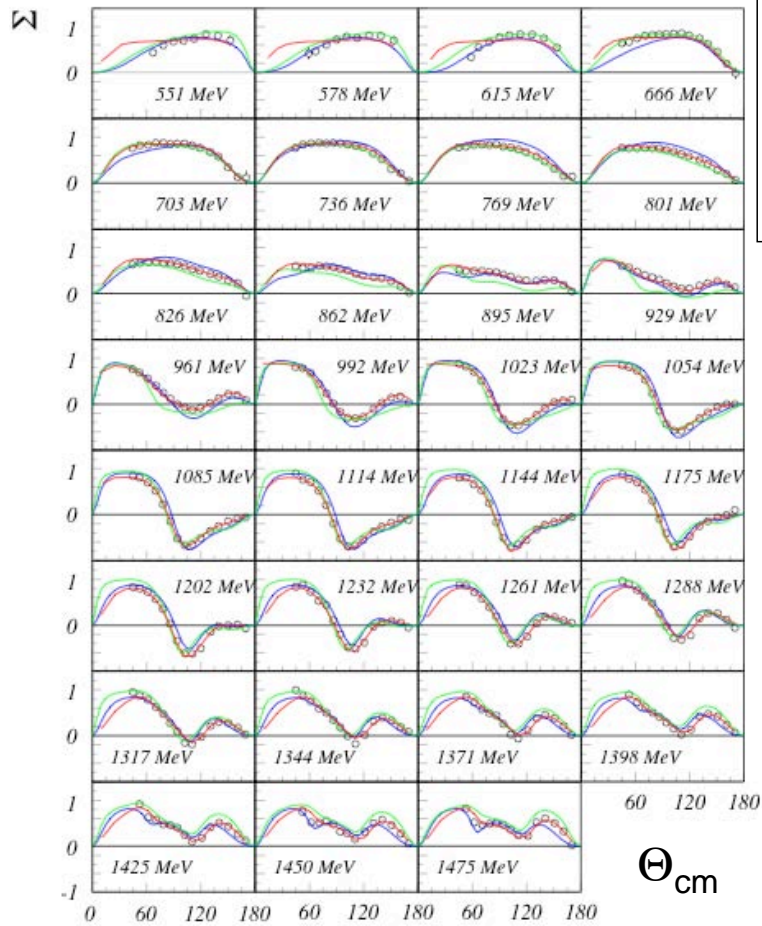
$$\frac{n_V - n_H}{n_V + n_H} = P_\gamma \Sigma \cos(2\varphi)$$

Green-UV data comparison

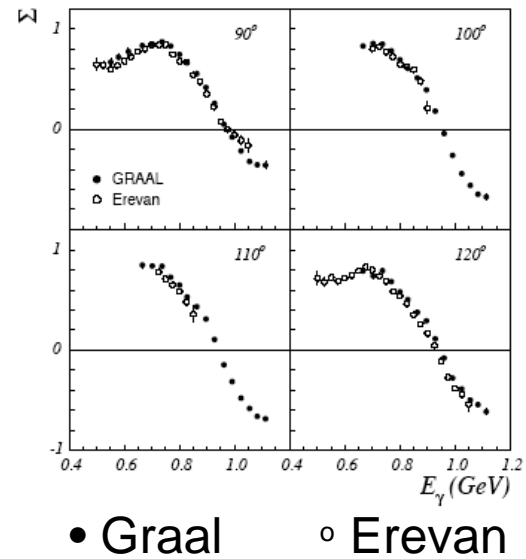


Comparison of the data obtained with the Green laser line and the UV. The different laser lines produce γ -ray spectra with different intensities and polarizations.

$$\vec{\gamma} + p \leftrightarrow p + \pi^0$$



— SAID-FA04 Erevan Σ + Bonn $d\sigma$
 — MAID2005 Bonn $d\sigma$ + Graal Σ
 — Bonn2005 $\pi N + \eta N + K\Lambda$
 + $K\Sigma$ + Graal Σ



π^0 Σ for free and quasi-free proton

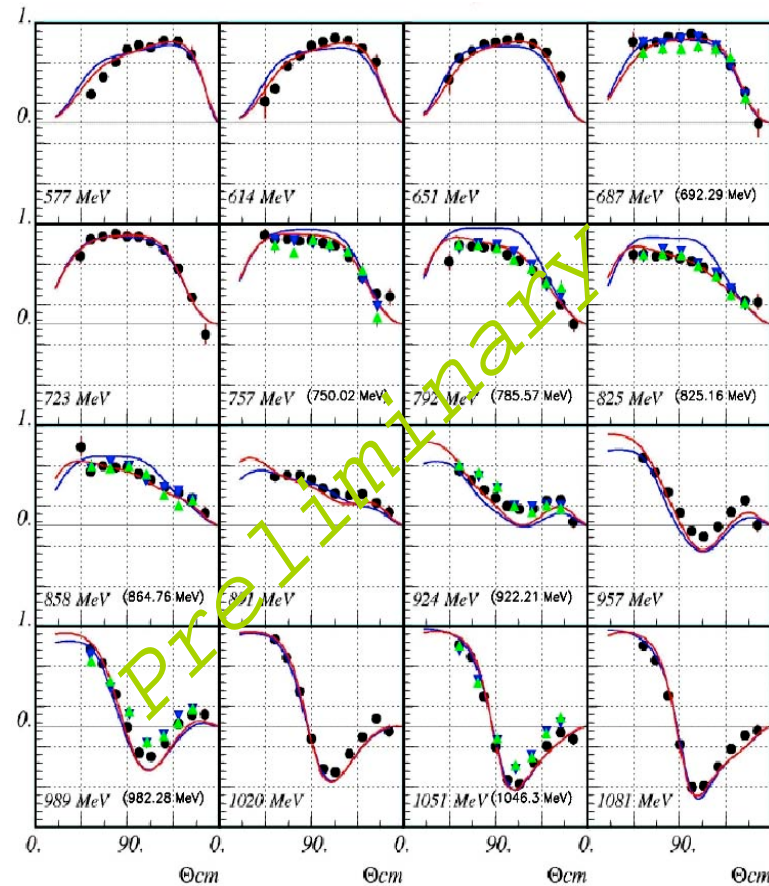
▼ Quasi-free proton (uv data)
 $\gamma + p + (n) \rightarrow \pi^0 + p + (n)$

▲ Quasi-free proton (green)
 $\gamma + p + (n) \rightarrow \pi^0 + p + (n)$

• Free proton
 $\gamma + p \rightarrow \pi^0 + p$

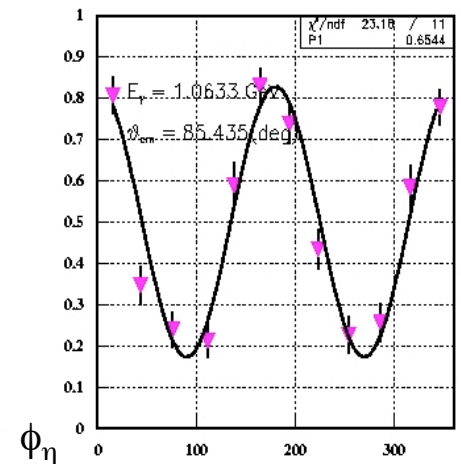
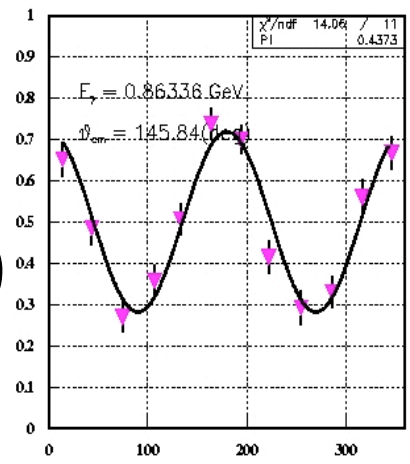
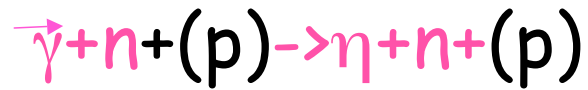
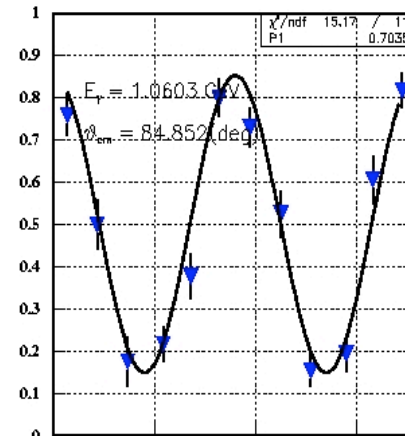
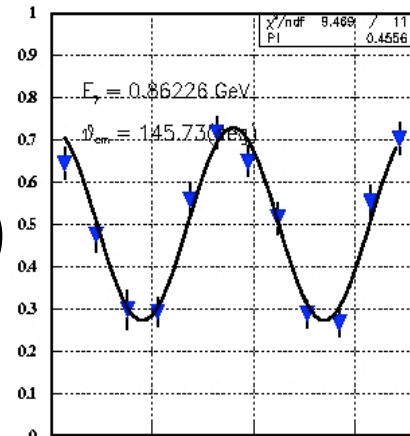
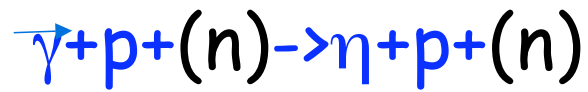
— Said WI00 (free proton)
 GRAAL data are not included

— Said FA01 (free proton)
 GRAAL data up to 1100 MeV
 are included



Azimuthal Distribution:

$$\frac{N_1 / K_1}{N_1 / K_1 + N_2 / K_2} = \frac{1}{2} \cdot (1 + P \Sigma \cos(2\phi))$$



The Virtex Fast Acquisition System 1/7

Authors List

Matteo Beretta
Laboratori Nazionali di Frascati, INFN

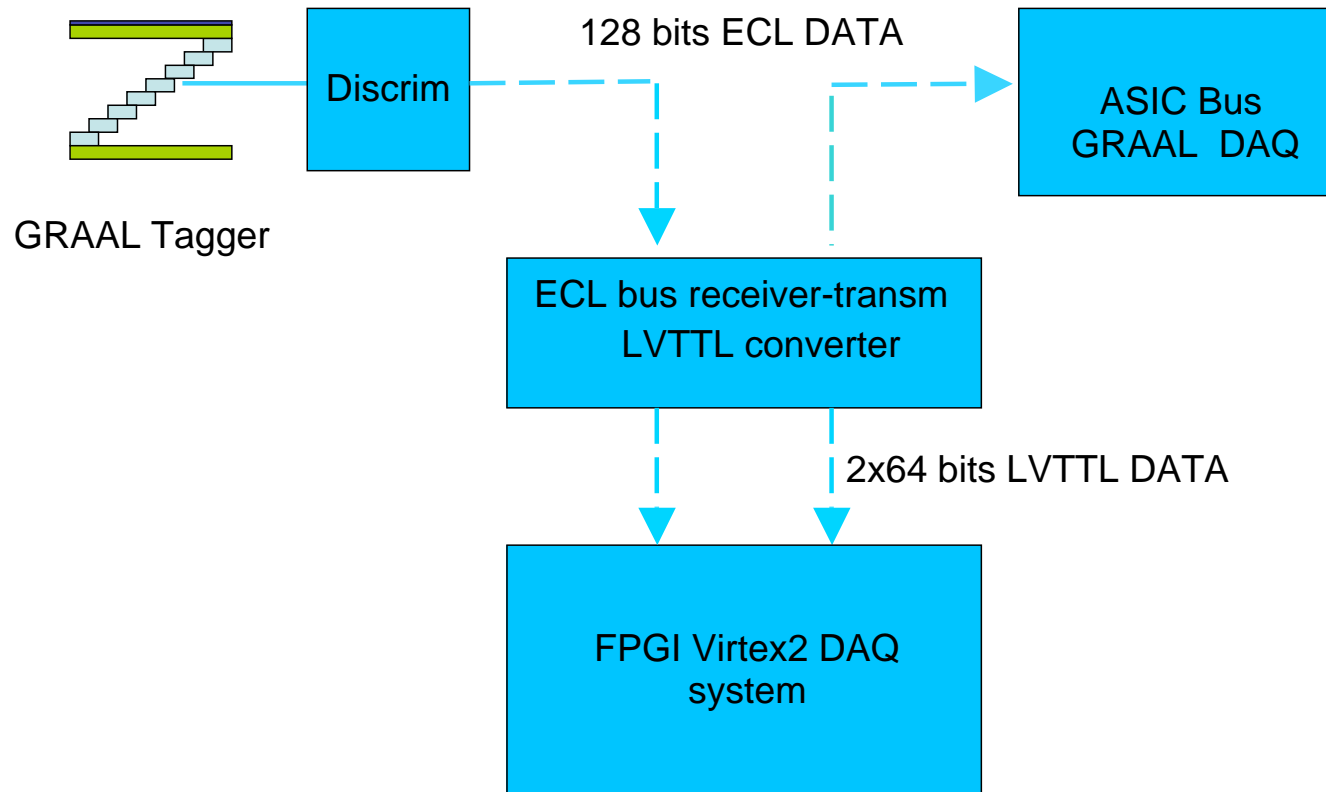
Roberto Messi
Dipartimento di Fisica, Università di Roma “Tor Vergata”
and
Sezione di Roma Tor Vergata, INFN

Dario Moricciani
Sezione di Roma Tor Vergata, INFN

Simone Angeloni
Dipartimento di Fisica, Università di Roma “Tor Vergata”

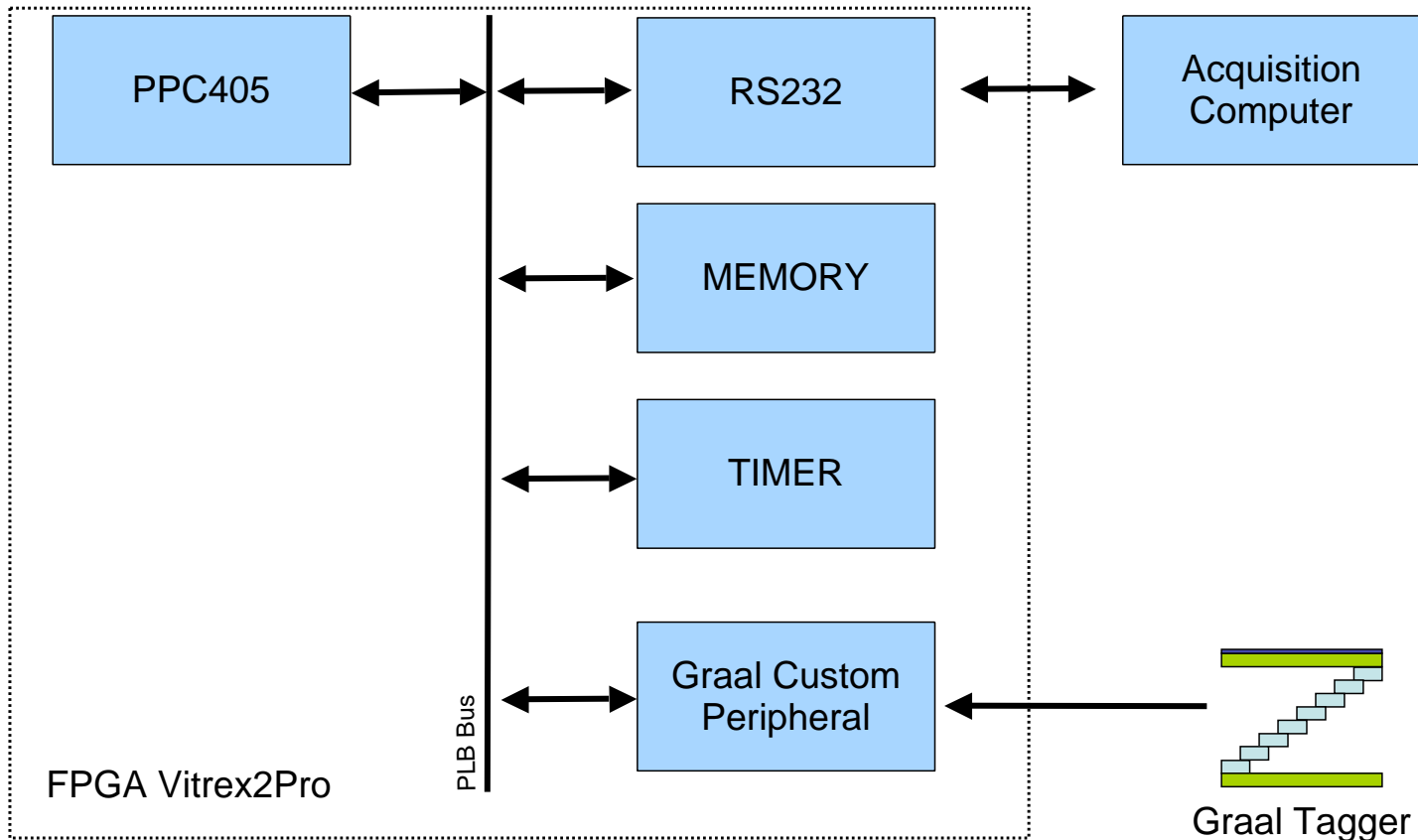
The Virtex Fast Acquisition System 2/7

General Set-up



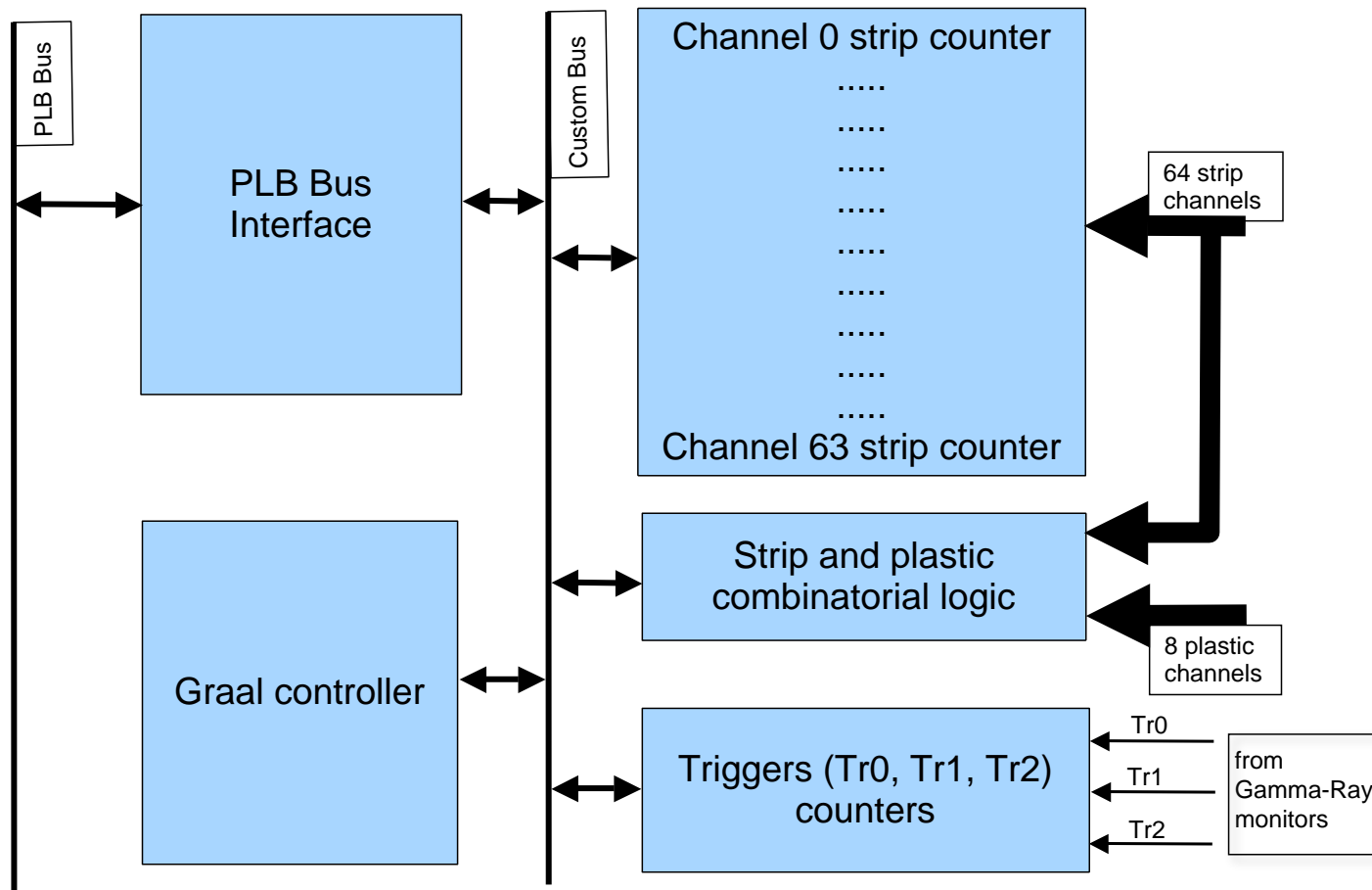
The Virtex Fast Acquisition System 3/7

Acquisition System



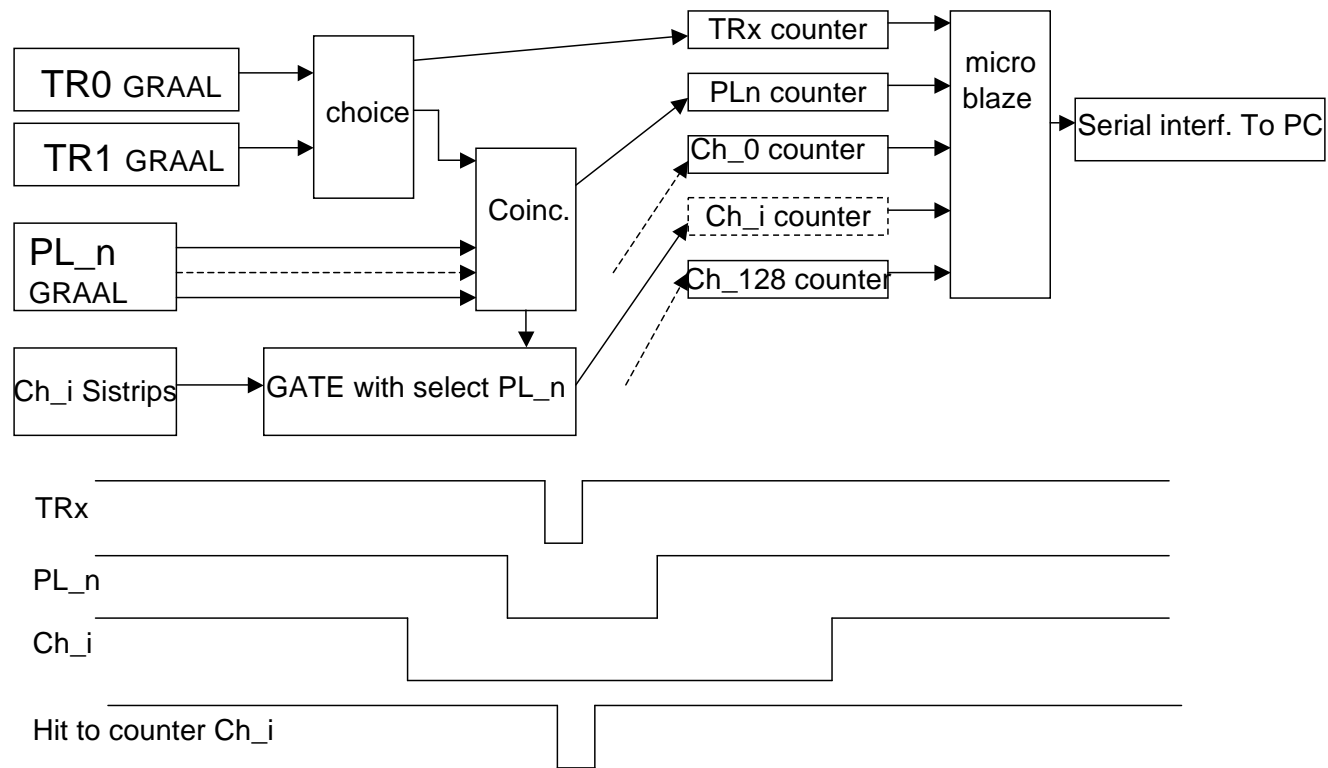
The Virtex Fast Acquisition System 4/7

Graal Custom Peripheral



The Virtex Fast Acquisition System 5/7

Coincidences and timing



The Virtex Fast Acquisition System 6/7

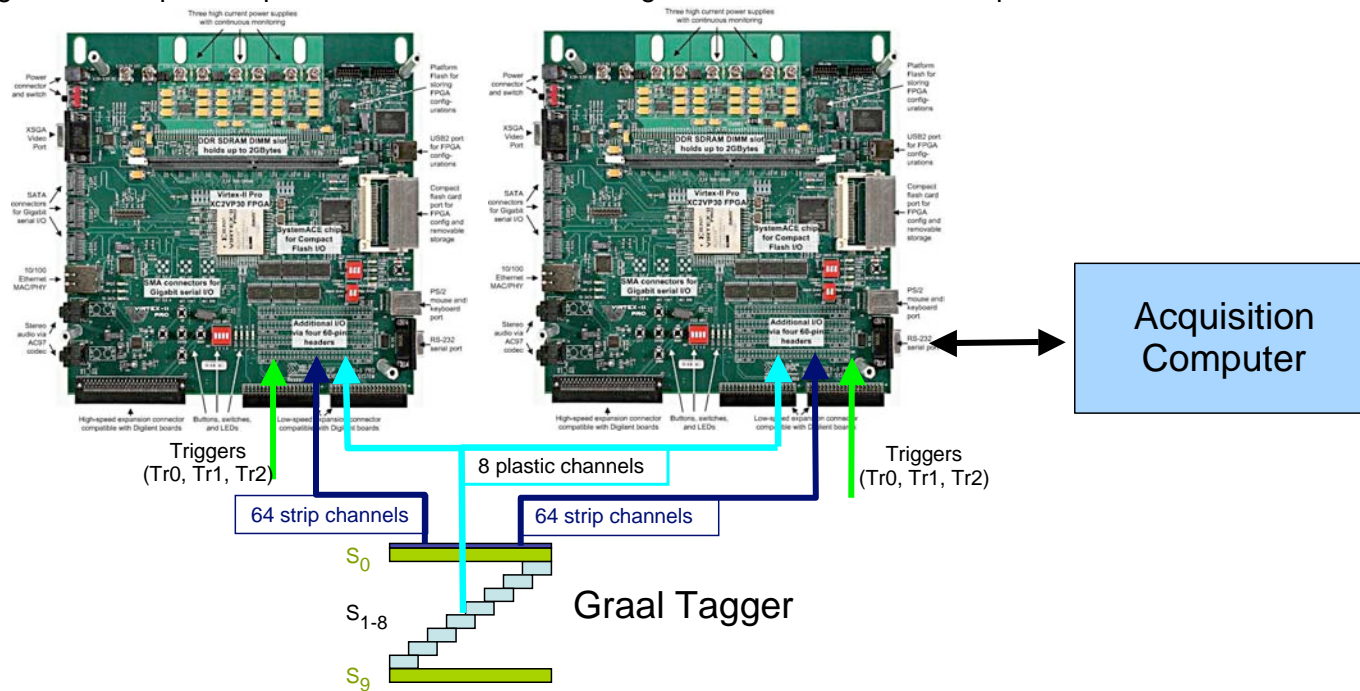
Key Features

Virtex-II Pro XC2VP30 FPGA with 30,816 Logic Cells, 136 18-bit multipliers, 2,448 Kb of block RAM, and two PowerPC Processors

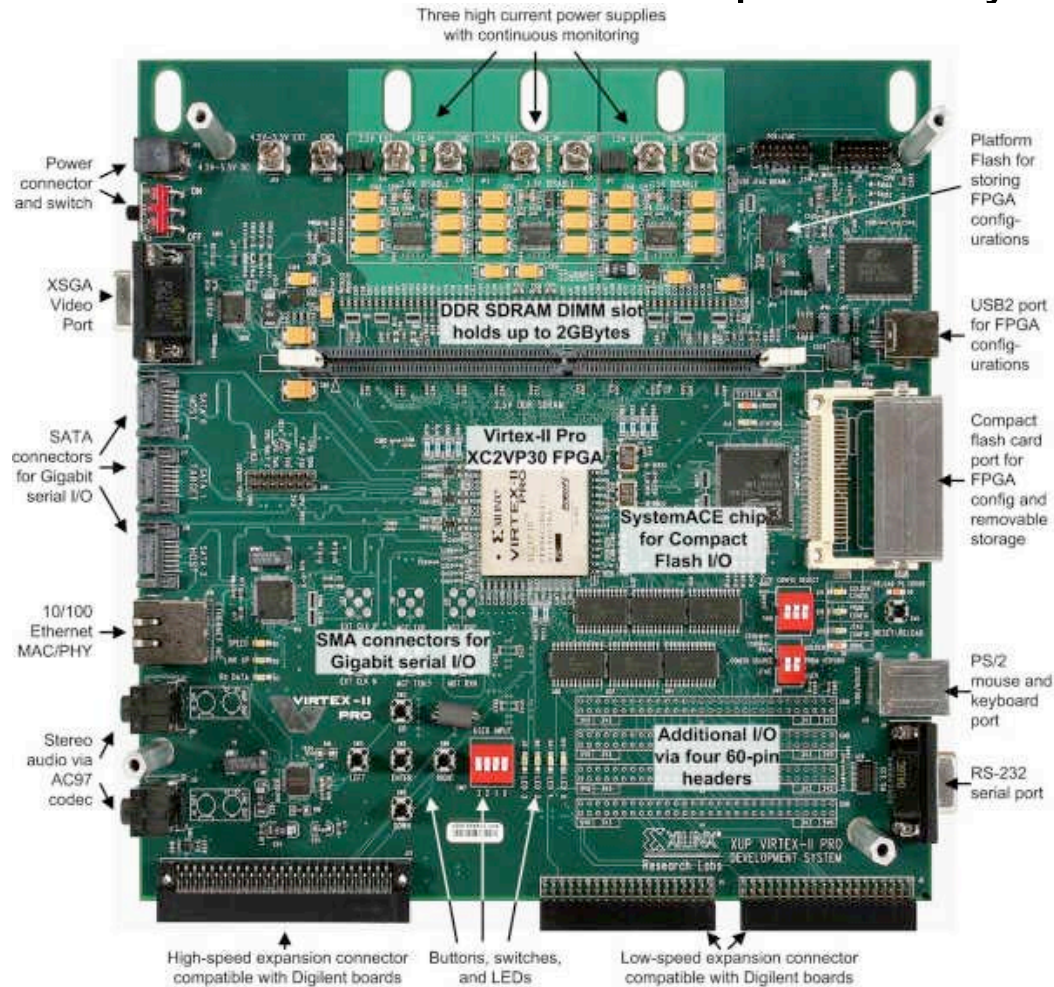
RS-232 ports

User GPIO (4 DIP switches, 5 push buttons, 4 LEDs)

High and low speed expansion connectors with a large collection of available expansion boards



The Virtex Fast Acquisition System 7/7

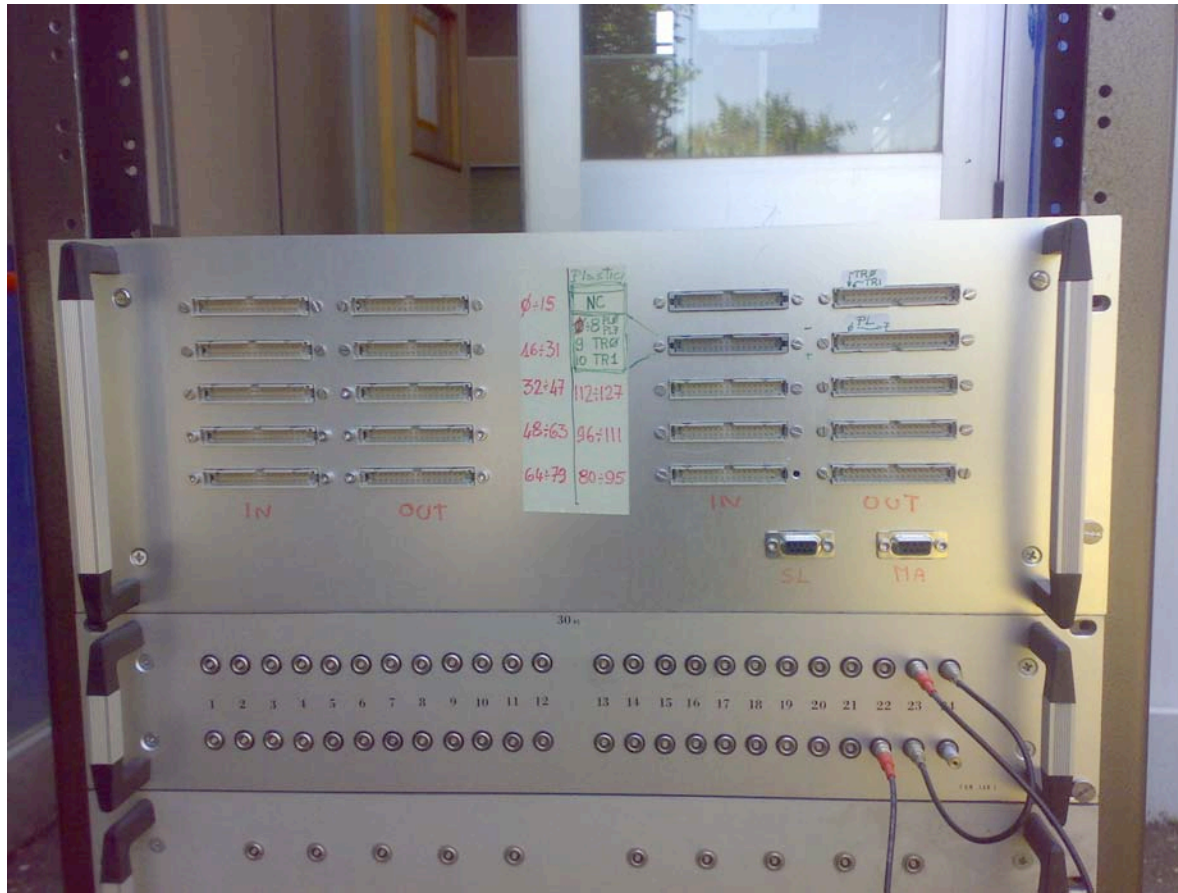


6/26/09

Carlo Schaefer Yerevan 1/06/09

52

Foto Virtex Front

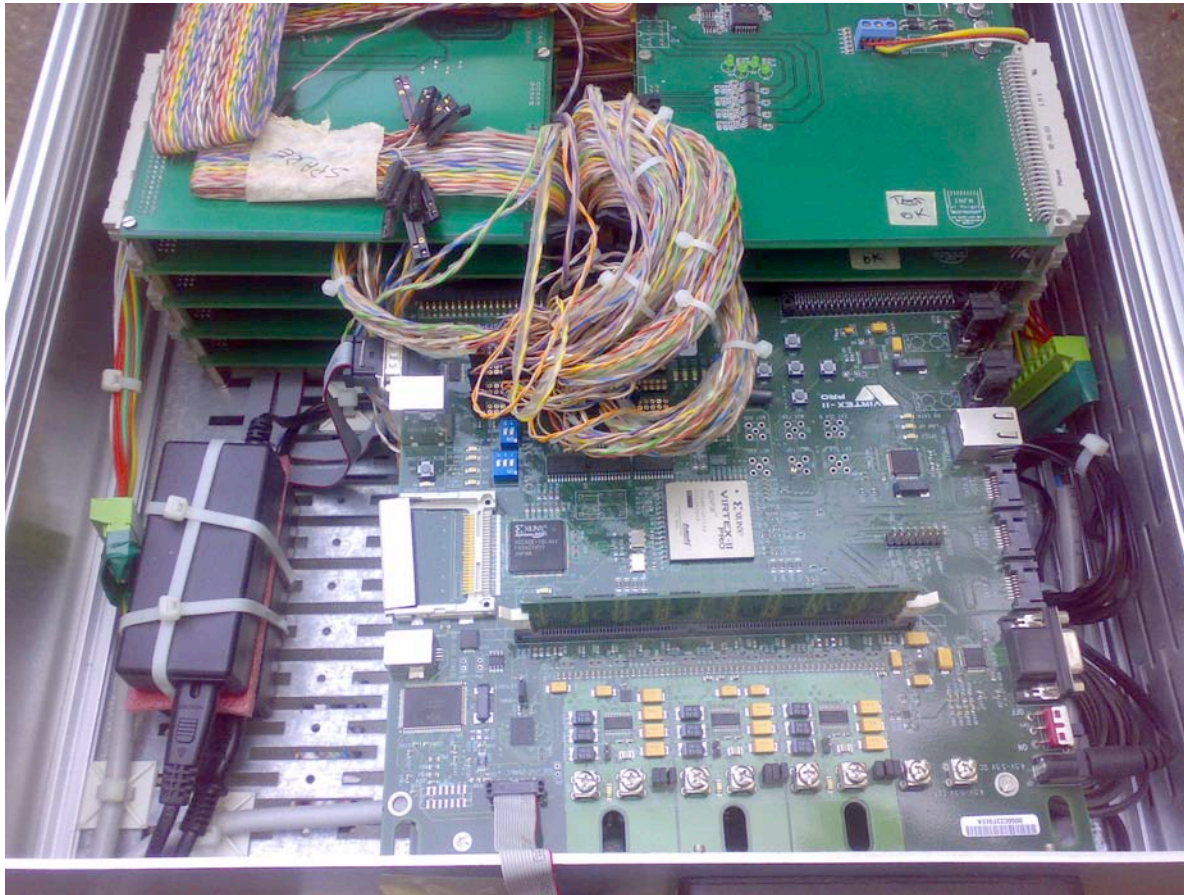


6/26/09

Carlo Schaerf Yerevan 1/06/09

53

Foto Virtex Open



6/26/09

Carlo Schaerf Yerevan 1/06/09

54

Counting Rate

The new electronics can work at an acquisition rate of 3 MHz. It has been installed in parallel with the old one allowing the simultaneous operation of the standard Graal acquisition system for the study of photonuclear reaction at the old rate of approximately 1 kHz and simultaneously the acquisition of the data from the tagging detector at the full intensity of the scattered electrons: up to 800 kHz. In this way it has been possible to acquire one spectrum of the tagged gamma rays in approximately 30 seconds while the old system needed approximately two hours to collect a spectrum with lower statistics.

As a result we have evidenced several characteristics of our detector that were averaged out before. In particular we have evidenced a very regular displacement of the detector due to the thermal oscillations of our apparatus due to the regular variations of the intensity of the electrons stored in the ring. This variations have been shown in a previous slide. A variation of the electron current from 210 to 160 mA did produce a variation of the temperature inside the tagging box of approximately 0.8 degree Centigrade which produced a displacement of the Compton edge by approximately 25 microns. Fortunately these variations were very regular and reproducible and could be corrected with a semi-empirical formula.

Collected Data

In conclusion with the new electronics we have collected:

July 2008	with the UV lines	14765	Spectra
November 2008	with the Green line	18621	Spectra
TOTAL		33386	Spectra

Under very stable conditions.